chemosensors

Review

Advances in MXene-Based Hybrids for Electrochemical Health Monitoring

Kandaswamy Theyagarajan [1,2,*] and Young-Joon Kim [1,2,*]

[1] Department of Electronic Engineering, Gachon University, Seongnam 13120, Gyeonggi-Do, Republic of Korea
[2] Department of Semiconductor Engineering, Gachon University, Seongnam 13120, Gyeonggi-Do, Republic of Korea
* Correspondence: thektr@gachon.ac.kr (K.T.); youngkim@gachon.ac.kr (Y.-J.K.)

Abstract

The growing demand for advanced health-monitoring technologies has intensified the need for early diagnosis of incurable diseases and timely detection of life-threatening conditions. Among various detection modalities, electrochemical sensing has emerged as a particularly promising approach due to its simplicity, cost-effectiveness, high sensitivity, rapid response, ease of miniaturization, and compatibility with portable, wearable, and implantable platforms. The performance of electrochemical sensors is strongly governed by the morphology and physicochemical properties of electrode materials. In this context, MXenes, 2D transition-metal carbides, nitrides, and carbonitrides have attracted increasing attention for sensing applications owing to their high electrical conductivity, large surface area, hydrophilicity, and rich surface chemistry. However, their practical implementation is hindered by oxidation and environmental instability, while surface modification strategies, although improving stability, may compromise intrinsic electrochemical activity and biocompatibility. Notably, MXene-based hybrids consistently demonstrate enhanced sensing performance, underscoring their potential for flexible and wearable electrochemical devices. Despite rapid progress in this field, a comprehensive review addressing the significance of MXene hybrids, their structure–property–performance relationships, and their role in electrochemical detection remains limited. Therefore, this review summarizes recent advances in MXene-based hybrid materials for electrochemical sensing and biosensing of biologically relevant analytes, with an emphasis on design strategies, functional enhancements, and their prospects for next-generation health-monitoring technologies.

Keywords: electrochemical sensor; biosensor; modified electrode; nanohybrids; nanomaterials

1. Introduction

In recent years, the rapid evolution of healthcare technologies has accelerated the transition from conventional clinical diagnostics toward personalized, preventive, and continuous health monitoring [1,2]. The increasing global burden of chronic and infectious diseases such as diabetes, cardiovascular disorders, cancer, and neurodegenerative conditions has underscored the need for early detection and real-time monitoring of physiological biomarkers [3–6]. Timely identification of abnormal biochemical changes enables early intervention, reduces morbidity and healthcare costs, and improves patients' overall quality of life [7]. Consequently, the development of portable, noninvasive, and highly sensitive diagnostic platforms has become a central objective in modern healthcare [7,8].

Received: 21 November 2025
Revised: 17 December 2025
Accepted: 22 December 2025
Published: 23 December 2025

Traditional laboratory-based diagnostic methods, including enzyme-linked immunosorbent assays (ELISA), chromatography, and spectroscopic techniques, though highly accurate, are constrained by complex instrumentation, high operational costs, lengthy procedures, and the requirement for trained personnel [9–11]. These limitations restrict their applicability in decentralized and point-of-care (POC) settings. Compared with optical, fluorescent, and colorimetric platforms, electrochemical sensors offer simpler instrumentation, easier miniaturization, and greater compatibility with low-power portable electronics [12–14]. In addition, electrochemical sensing technologies have gained significant attention due to their inherent advantages, including low cost, ease of operation, high sensitivity, rapid response, and compatibility with wearable and implantable devices [15,16]. Electrochemical sensors transduce chemical or biological interactions at the electrode–electrolyte interface into quantifiable electrical signals, enabling real-time insight into physiological processes [17]. Additionally, their low sample-volume requirements make them highly suitable for POC testing, one-drop analysis and microvolume assays, and in situ, on-the-go monitoring of clinically and environmentally relevant analytes [18–20].

The performance of electrochemical sensors is primarily dictated by the properties of their electrode surfaces, which govern electron-transfer kinetics, electrocatalytic activity, and analyte interactions [21,22]. To enhance these characteristics, surface modification strategies have evolved from the use of traditional materials such as carbon pastes and noble metals to advanced nanomaterials that offer superior conductivity, large electroactive surface areas, multidimensional architectures, tunable porosity and tailored surface functionalities [23–26]. Over the past decade, two-dimensional (2D) materials, notably graphene, carbon nanotubes, and transition-metal dichalcogenides, have revolutionized electrochemical biosensing due to their high surface area, excellent conductivity, abundant catalytic sites, cost-effectiveness, and synthetic versatility [27,28]. Nonetheless, these materials still face challenges, including limited long-term stability, susceptibility to surface oxidation, reduced catalytic activity, and insufficient active sites for biomolecule immobilization and stabilization [29].

In this context, MXenes (MXs), a rapidly expanding family of 2D transition-metal carbides, nitrides, and carbonitrides produced through selective etching of the A-layer from MAX phases, have emerged as a next-generation platform for high-performance electrochemical sensors and biosensors [30,31]. The A layer can consist of elements such as Al, Si, As, P, S, In, Ga, Ge or Sn; however, Al is the most commonly preferred A-layer element as it can be easily removed under relatively mild etching conditions. MXs, typically represented by the formula $M_{n+1}X_nT_x$ (where M is an early transition metal, X is carbon and/or nitrogen, and T_x denotes surface terminal groups such as oxygen, hydroxyls, or fluorine), were first reported in 2011 by Prof. Yury Gogotsi and colleagues [32]. Since then, they have attracted immense research interest due to their metallic-like conductivity, hydrophilic nature, tunable surface chemistry, mechanical robustness, and large specific surface area [33,34]. These features make MXs particularly attractive for biosensing applications, where rapid charge transfer and effective biomolecule immobilization are essential for signal amplification and enhanced sensitivity. Moreover, MXs exhibit remarkable biocompatibility and mechanical flexibility, offering significant potential for wearable and implantable health-monitoring systems [35]. However, pristine MXs are prone to oxidation, particularly under humid, aqueous, or physiological conditions, which can severely limit their operational lifetime, reproducibility, and long-term reliability in electrochemical sensing applications. In addition to oxidation, pristine MXs often suffer from layer restacking, reduced structural stability, and uncontrolled surface chemistry evolution during operation [36]. To address these limitations, multiple strategies, including doping, composite formation, and hybridization, have been explored using diverse materials such as carbon nanostructures, metal and

covalent organic frameworks, metal nanoparticles, metal oxides, polymers, and layered hydroxides [37–39]. While surface modification and hybridization strategies are widely employed to enhance MX stability and facilitate hybrid formation, they often represent a double-edged sword. Specifically, capping, or consuming surface hydroxyl and other terminal groups through processes such as silanization, polymer grafting, or inorganic coating can reduce hydrophilicity, restrict ion accessibility, and passivate electrochemically active sites, thereby diminishing functional-group-driven electrochemical activity. Although many studies report improved stability and sensing performance, the potential loss of intrinsic MX activity due to surface passivation is frequently underemphasized and warrants careful consideration. A graphical representation of various steps involved in the fabrication of MX hybrids is shown in Figure 1. These hybrid systems harness synergistic effects by combining the high conductivity and surface activity of MXs with the stability, selectivity, and catalytic properties of complementary materials. As a result, MX-based hybrids demonstrate remarkable improvements in sensor performance metrics, including enhanced sensitivity, improved anti-interference capability, lower detection limits, and superior operational stability, making them ideal candidates for continuous health monitoring and POC diagnostics [40–42]. In addition, for biosensing and tissue-interfacing applications, the biocompatibility and degradation pathways of MX-based systems must be carefully considered. When MXs are operated under minimally fluidic conditions, they can remain relatively stable, hydrogel-based and continuously wetted MX architectures are more susceptible to oxidative degradation into transition-metal oxides. Notably, Ti-based MXs generally present a lower toxicity risk upon degradation compared to V-based MXs, which may decompose into highly toxic V_2O_5, raising concerns for long-term biointegration and clinical translation. Therefore, rational MX composition selection, degradation control, and comprehensive biosafety evaluation are critical for the successful clinical deployment of MX-based bioelectronic systems.

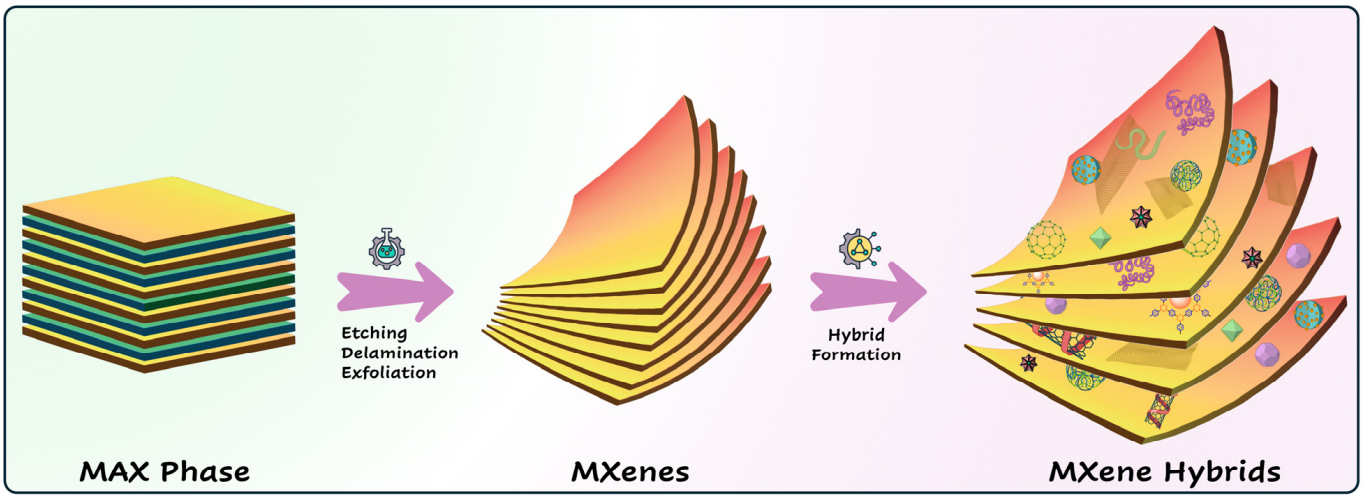

Figure 1. Graphical illustration of the stepwise synthesis of MXene nanosheets and their corresponding hybrid structures. The icons used in this image were adapted from flaticon.com and BioRender. Kim, Y. (2025) https://BioRender.com/50bzbi8, accessed on 20 November 2025.

Despite growing interest in MX-based hybrids for electrochemical sensing, comprehensive analyses of their applications in health monitoring, underlying mechanisms, structure–property–performance relationships, and existing challenges remain limited. Therefore, this review aims to provide an in-depth overview of recent advances in MX-based hybrids for the electrochemical detection of physiologically relevant biomarkers and biologically significant chemicals. Emphasis is placed on their design strategies, functionalization approaches,

sensing mechanisms, and integration into wearable and portable health-monitoring systems. Finally, the review highlights current challenges and future perspectives for translating MX-hybrid based electrochemical sensors from laboratory prototypes to practical tools for clinical and personalized healthcare.

2. MXene Hybrid Based Electrochemical Sensors

2.1. MXene-Carbon Nanostructure Hybrids

Carbon nanostructures (CNs) are materials composed entirely or predominantly of carbon, with at least one dimension in the nanoscale range. They include carbon nanotubes (CNTs), graphene (GR) and its derivatives, carbon quantum dots, carbon nanofibers and several other forms. These materials possess unique chemical, electrical, optical, mechanical and thermal properties [43,44]. In addition, they offer a large surface area, abundant surface functional groups, excellent synthetic versatility, ease of functionalization, cost-effectiveness, and good biocompatibility, and they can even be synthesized from various waste materials. In modern technology, CNs have found widespread applications in catalysis (bio/electro/chemical), energy storage (batteries, supercapacitors, etc.), sensing (chemical and biological) and surface coatings. Incorporating these CNs into MX nanosheets prevent layer restacking by acting as spacers, enhances chemical stability, maintains interlayer spacing, increases surface area, ion diffusion, and mass transport, improves dispersibility, augments electrical and chemical properties, and enhances the surface functionality of MX nanosheets [45]. Some commonly used CNs for MX hybrid formation and their electrochemical responses toward biologically significant analytes are discussed below.

Using a simple ultrasound-assisted synthesis method, a GR@MX hybrid was prepared and subsequently utilized for the electrochemical sensing of rhodamine B and chlorpromazine [46]. Chlorpromazine is an antipsychotic drug that is sometimes illegally used in livestock farming, while rhodamine B is a synthetic dye often misused as a food colorant. Both compounds are associated with serious adverse effects, including tardive dyskinesia, neuroleptic malignant syndrome and carcinogenicity. In this work, GR and MX nanosheets were individually exfoliated via solution-phase exfoliation using N-methylpyrrolidone and then ultrasonically mixed in different proportions to obtain the GR@MX hybrids (Figure 2A). Compared to other synthetic routes, solution-phase exfoliation is a cost-effective, eco-friendly and non-toxic method that avoids the use of hazardous chemicals. Furthermore, the hybrids synthesized by this approach exhibited excellent adsorption capacity, enhanced electron transfer, and superior electrocatalytic activity. These properties govern the sensing mechanism at the electrode–electrolyte interface. The surface-terminated MX enables strong adsorption and preconcentration of both analytes; meanwhile, the conductive graphene network enhances electron transport and reduces charge transfer resistance. Their synergistic coupling suppresses restacking, maintains a high electroactive surface area, and accelerates oxidation kinetics, resulting in highly sensitive detection of both analytes. In an interesting study by Gu and colleagues, a three-dimensional (3D) porous MX-GR hybrid was fabricated via an ultrasonic mixing and rapid drying process, which was then employed for the enzymatic detection of glucose [47]. The selective and sensitive detection of glucose from various bodily fluids is critically important for effective diabetes management. The 3D porous architecture was generated through the crosslinking of MX and GR sheets, and its pore structure could be tuned simply by adjusting the weight ratio of the MX and GR mixture. An increase in GR content enhanced the porosity of the resulting hybrids. The internal pores thus formed effectively preserved the native structure and activity of the immobilized glucose oxidase enzymes and augmented their

electrocatalytic performance towards glucose oxidation. The stepwise synthesis of MX and fabrication of MX-GR based glucose sensor are illustrated in Figure 2B.

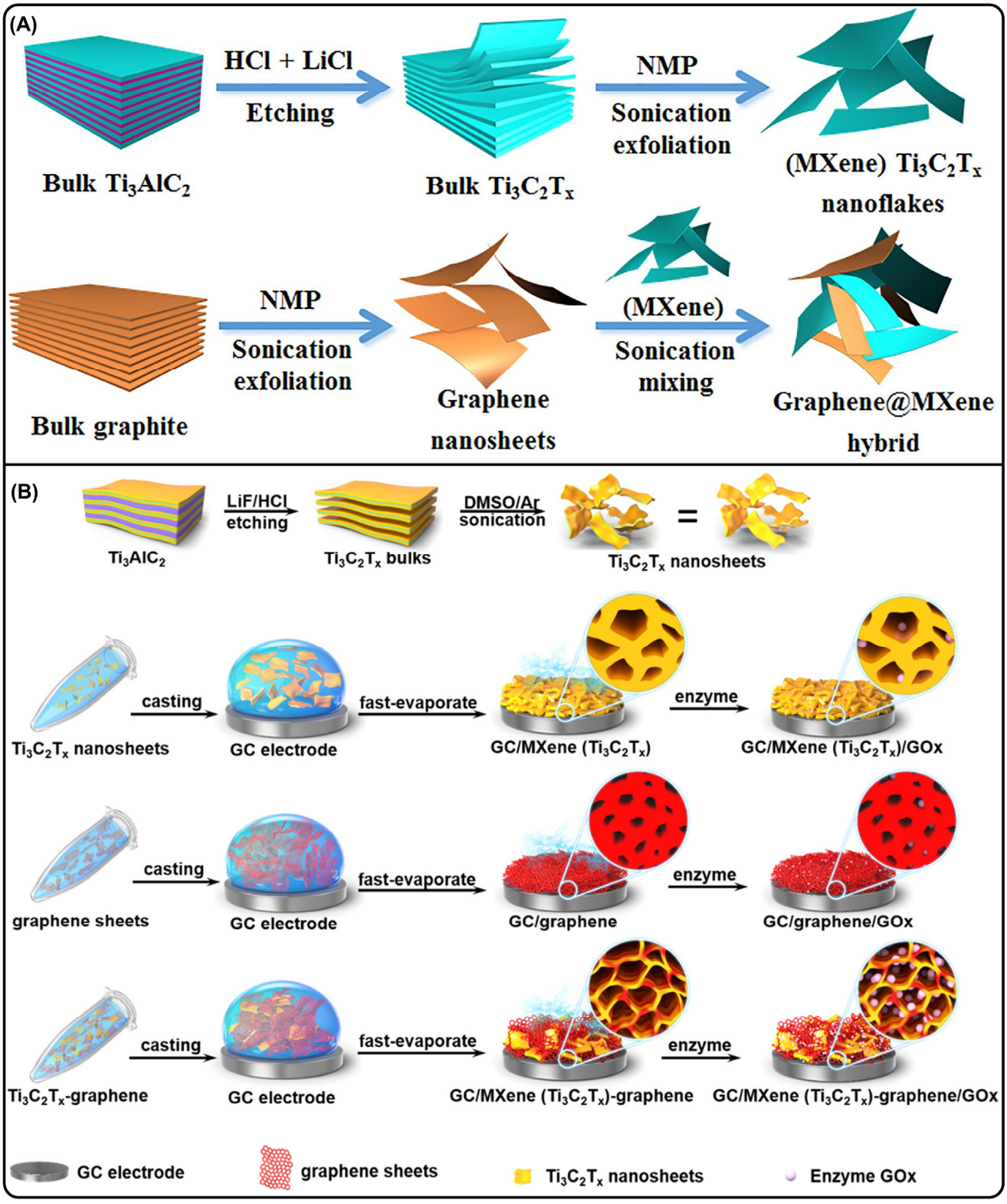

Figure 2. (**A**) Schematic representation of the stepwise fabrication of GR@MX hybrid. Reproduced with permission from [46]. (**B**) Graphical illustration of the stepwise synthesis of MX and the fabrication of MX/GR/GOx based glucose sensor. Reproduced with permission from [47].

Similarly, in another study, an MX-GR hybrid synthesized via a top-down approach was employed for the electrochemical detection of nicotine [48]. Nicotine is a toxic and addictive compound derived from tobacco plants that causes various diseases, including lung cancer and neurodegenerative disorders. Compared to the previous study, this work utilized equivalent amounts of MX and GR in the hybrid formation. Moreover, the fabricated sensor successfully quantified nicotine in both artificial and human saliva samples. From the same research group, another MX-GR hybrid was constructed using a similar methodology and applied for the selective sensing of bisphenol A from plastic products [49]. Bisphenol A is an endocrine-disrupting chemical known to interfere with hormonal activity and is associated with several health risks, including cancers, infertility, impaired brain development, and cardiovascular diseases. An ultrasonication-assisted synthesis of MX-embedded graphite nanoplatelets was utilized for the selective quantification of thiamethoxam [50]. Thiamethoxam is a neonicotinoid insecticide widely used in agriculture to control a broad spectrum of pests; however, its exposure is associated with several adverse effects, including nerve damage, endocrine disruption, and carcinogenicity. The developed sensor effectively quantified thiamethoxam in beekeeping products and the recovery values were comparable to those obtained using chromatographic methods. In another work, a polyelectrolyte-modified MX-graphene oxide (GO) hybrid was fabricated for the selective detection of furazolidone [51]. Furazolidone is a nitrofuran antimicrobial agent used to treat bacterial and protozoal infections and is also utilized in livestock feed; however, it exhibits serious adverse effects, including mutagenic, teratogenic and carcinogenic properties. Initially, an MX-GO colloidal solution was formed and subsequently mixed with poly(diallyldimethylammonium chloride) polymer, which was then deposited onto a screen printed electrode (SPE) to construct the proposed sensor. The incorporation of the polyelectrolyte prevented the aggregation of MX and GO, increased the surface area, provided abundant active sites, and enhanced electron transfer efficiency.

A nanohybrid composed of MX and single-walled carbon nanotubes (SWCNT) was fabricated via ultrasonication and employed for monitoring serotonin release from 4T1 and human umbilical vein endothelial cells [52]. The incorporated SWCNTs were uniformly distributed over and between the MX nanosheets, effectively preventing aggregation, enhancing electrical conductivity, exposing additional active sites, and improving the overall electrocatalytic performance of the developed nanohybrid. The sensor successfully quantified the serotonin released from both cell lines with excellent recovery values. Similarly, a holey multiwalled carbon nanotube (h-MWCNTs) decorated sulphur- and nitrogen-co-doped vanadium carbide (S,N-V_2C) MX nanohybrid was developed for the selective detection of nicotine [53]. Using a template-free synthesis approach, S,N-V_2C nanoflowers were produced via ultrasonication followed by freeze-drying, after which they were decorated with h-MWCNTs to enhance oxidation stability and prevent agglomeration. Furthermore, controlled "hole" formation on the MWCNTs improved their printability and electrochemical activity. The resulting nanohybrid ink was inkjet-printed onto a flexible substrate and utilized for nicotine detection in artificial urine samples. Table 1 compares the electrochemical performance of various MX-carbon nanostructure based hybrids.

Table 1. Electrochemical performance comparisons of various MX-carbon nanostructure hybrids.

Sensor	Analyte	Linear Range (μM)	LOD (μM)	Sensitivity	Real Sample	Ref.
GR@Ti-MX	Chlorpromazine Rhodamine B	5×10^{-3}–0.5 1×10^{-2}–2.5	1.2×10^{-3} 2.4×10^{-3}	1090 μA μM^{-1} cm^{-2} 440 & 102.14 μA μM^{-1} cm^{-2}	Pork, chili powder	[46]

Table 1. *Cont.*

Sensor	Analyte	Linear Range (μM)	LOD (μM)	Sensitivity	Real Sample	Ref.
GOx/GR-Ti-MX/GCE	Glucose	2×10^2–5.5×10^3	0.66 0.98	12 μA μM^{-1} 20.16 μA μM^{-1}	Human blood serum	[47]
GR/MX/GCE	Nicotine	1–55 3×10^{-2}–0.6	2.9×10^{-4} 2.8×10^{-4}	3.5 μA μM^{-1} cm^{-2} 0.527 μA μM^{-1} cm^{-2}	Human saliva, artificial saliva	[48]
GR/MX/GCE	Bisphenol	1×10^{-3}–0.18 1–10	0.048 0.35	0.0124 μA μM^{-1} 0.0419 nA μM^{-1}	Water bottles, baby feeding bottles, food package	[49]
xGnP/Ti-MX/GCE	Thiamethoxan	0.048–30	0.02	6.57 μA μmol. L^{-1}	Honeycomb, mead	[50]
GO-MX	Furazolidone	0.04–200	1.2×10^{-3}	27.6836 μA μM^{-1} cm^{-2}	Pipe water, river water	[51]
MX-SWCNTs/GCE	Serotonin	0.04–103.2	1×10^{-3}	-	Live cell monitoring	[52]
N,S-V_2C-MX/Nf/h-MWCNT	Nicotine	10–500	0.058	0.2353 μA μM^{-1}	Artificial urine, tobacco extract	[53]
Ti-MX/MWCNT/Valinomycin	K^+	(1–32) $\times 10^3$	-	63 mV dec^{-1}	Human sweat	[54]
Ti-MX/CNT/MoS_2	Chloramphenicol	8×10^{-3}–0.152	3.2×10^{-4}	14.22 μA nM^{-1} cm^{-2}	Milk, eye drops, pork	[55]

GOx—glucose oxidase; GR—Graphene; h-MWCNT—holey multiwalled carbon nanotube; MWCNT—Multiwalled carbon nanotube; SWCNT—single-walled carbon nanotube; xGnP—Exfoliated graphite nanoplates.

A fully integrated, battery-free, wireless, skin-interfaced electrochemical patch was developed by combining a microfluidic sweat-collection module with an ion-selective platform for potassium sensing in human sweat [54]. To enhance the electrode interface, a hybrid network of MWCNTs and Ti-MX was incorporated to increase surface area and charge-transfer efficiency, enabling strong immobilization of a valinomycin-based ion-selective membrane and facilitating rapid ion diffusion through the porous matrix. Near-field-communication technology enabled wireless data readout via a smartphone, while the integrated microfluidic channel efficiently collected sweat and prevented contamination of the sensing surface. Compared with earlier sweat-ion sensors, this system eliminates the need for an external power source, improves sensitivity through advanced nanomaterials, and leverages microfluidics for reliable in situ sampling. In another study, a ternary hybrid electrode was fabricated by growing layered MoS_2 nanoflakes on stacked Ti-MX sheets, followed by the incorporation of a CNT network for the selective sensing of chloramphenicol [55]. Acid etching of MX prevented layer restacking and created an interlayered architecture suitable for MoS_2 growth, thereby enhancing conductivity and structural robustness. The CNT network acted as an electron-transport pathway, increasing the electrochemical active surface area and stabilizing the overall structure. The resulting Ti-MX/MoS_2/CNT composite exhibited rapid electron-transport kinetics, numerous active sites, and a stable 3D architecture, enabling highly sensitive chloramphenicol detection. This work emphasizes the potential of integrating layered MX, transition-metal dichalcogenide nanoflakes, and CNTs to construct synergistic hybrid networks with enhanced conductivity, larger surface areas, and improved structural stability.

2.2. MXene–Metal Nanomaterial Hybrids

A Nb-MX based nanocomposite was engineered via amino-functionalization with (3-aminopropyl) triethoxysilane (APTES), followed by self-assembly of 10 nm gold nanoparticles (GNPs), forming an advanced hybrid for aptamer-based progesterone detection [56]. The fluorine-free NaOH etching route produced few-layer Nb-MX nanosheets with enhanced conductivity, hydrophilicity, and chemical stability. APTES not only stabilized MX sheets but also introduced amine functional groups, enabling uniform immobilization of GNPs and thereby increasing surface reactivity and enhancing electron transport efficiency. The GNPs-APTES-Nb-MX structure exhibited an enlarged electroactive area and excellent charge-transfer capability. This synergistic architecture enabled thiolated progesterone-specific aptamer anchoring and reliable redox signaling. Upon progesterone binding, it triggers aptamer conformational changes that hinder redox probe access and slow down electron transfer, resulting in a concentration-dependent decrease in voltammetric current for sensitive and selective detection of progesterone. Overall, the robust structural design highlights Nb-MX as a conductive and biocompatible scaffold with strong potential for next-generation electrochemical biosensors. In another study, a flexible, noninvasive electrochemical glucose sensor was developed using MX-Au nanocomposites integrated with a Janus polyurethane and polyvinyl alcohol (PVA) nanofiber membrane [57]. Here, Ti-MX served simultaneously as a conductive substrate and an in situ reducing agent for GNPs, resulting in uniformly dispersed GNPs on the MX surface without the need for external stabilizers. This hybrid exhibited superior electron transfer, expanded electroactive surface area, and peroxidase-like catalytic activity, making it ideal for glucose oxidase immobilization. The Janus membrane, fabricated via electrospinning, enabled unidirectional sweat transport through hydrophobic-hydrophilic asymmetry, ensuring efficient sample delivery and wearer comfort. The integration of catalytically active MX-Au with a moisture-guiding Janus interface demonstrates synergistic material architecture for high-performance wearable biosensing.

Similarly, an MX nanosheet-Au nanourchin hybrid was fabricated to mimic a superoxide dismutase and utilized for real-time detection of superoxide anions released from living cells [58]. Superoxide ($O_2^{\bullet -}$) is a critical reactive oxygen species, and its overproduction is strongly associated with oxidative stress–related pathologies, including inflammation, neurodegeneration, and cancer. The hybrid comprised a few-layer MX nanosheet scaffold decorated with abundant sharp-featured Au nanourchins (Figure 3). This configuration leveraged the high conductivity and large accessible surface area of MX together with the intrinsic catalytic activity of the Au nanourchins, which served as enzyme mimetics. The MX–Au architecture enhanced electron-transfer kinetics and expanded the electroactive surface, enabling efficient interaction with superoxide and enabling rapid, real-time monitoring. This sensor thus combines the strengths of a 2D conductive framework and nanostructured metal catalysts to achieve high sensitivity, fast response, and dynamic biological detection capability. A wearable electrochemical aptasensor was also developed for noninvasive monitoring of cortisol, a key stress hormone whose elevated levels are strongly linked to numerous adverse physical and psychological health outcomes [59]. The device was constructed by modifying a SPE with a hybrid of 2D MX nanosheets decorated with GNPs. The MX scaffold provides high conductivity and a large surface area, while the GNPs introduce abundant Au–S binding sites for immobilizing thiolated aptamers, thereby enhancing electron-transfer efficiency. This synergistic MX/GNP architecture increases the electroactive surface and supports dense loading of methylene-blue-tagged aptamers, thereby significantly improving sensitivity and selectivity for cortisol detection in sweat.

A sandwich-type electrochemical immunosensor was fabricated for the tumor marker CYFRA21-1 using a hybrid material platform comprising a 2D MX decorated with GNPs as

the electrode substrate and a signal tag built from a COF doped with GNPs and toluidine blue (TB) [60]. The MX/GNPs substrate enabled high antibody loading capacity and efficient electron transfer, while the TB-Au-COF nanolabel supplied abundant redox active units and secondary antibody binding sites, collectively boosting signal output. A related hybrid architecture was engineered, combining a few-layer MX decorated with in situ electrodeposited GNPs for the detection of amyloid-β oligomers, which are key biomarkers implicated in early-stage Alzheimer's disease, highlighting the investigative focus on these low-abundance species in clinical diagnostics [61]. In parallel, a signal probe composed of a COF embedding GNPs and a TB mediator improved electron-hole separation and charge-carrier utilization. The "double-amplification" strategy, employing both a conductive Au-MX substrate and an Au@COF/TB signal tag, delivered an ultralow detection limit and a broad dynamic range, demonstrating a highly sensitive platform for early Alzheimer's diagnostics. From a materials perspective, both sensing systems utilize MX + COF hybrids to enhance electrochemical transduction, yet the latter advances the concept by (i) applying it to a neurological biomarker and (ii) implementing dual amplification, illustrating the progression of MX–COF composite design toward ultrasensitive biosensing. The same MX-Au hybrid strategy was extended towards a biomarker, cardiac troponin I, a key biomarker of myocardial infarction and cardiac stress [62]. Here, the hybrid served as an efficient immobilization matrix for a tetrahedral DNA aptamer scaffold, ensuring ordered probe orientation and enhanced signal transduction. The incorporation of an in situ hybrid chain reaction provided robust amplification, while the Au-S anchoring improved interfacial stability. Overall, this work underscores the versatility of MX–Au hybrids in enabling high-performance biosensing across diverse biomedical analytes. In another study, a one-pot synthesis was used to prepare a heterostructure composed of 2D MX nanosheets doped with GNPs, leveraging the high electrical conductivity of MX and the catalytic and biomolecule-anchoring capabilities of GNPs [63]. The resulting hybrid was employed as an electrode platform on an SPE for simultaneous ultrasensitive electrochemical detection of an antibiotic (ampicillin) and a mycotoxin (fumonisin B1). The material design highlights the synergy between the sheet-like, highly conductive MX scaffold and GNPs, which enhance surface area, promote efficient biomolecule immobilization, and accelerate electron-transfer kinetics. From a materials perspective, both [62,63] utilize MX hybridized with GNPs to boost signal transduction. However, the former achieves amplification primarily through DNA nanostructures and hybrid chain reaction based biological amplification, whereas the latter focuses on intrinsic material engineering using MX/GNP heterostructures themselves as the amplification mechanism rather than relying on complex biochemical cascades. This distinction underscores two complementary strategies for achieving high sensitivity: biological amplification versus architecturally driven material-based amplification.

A portable electrochemical sensor was built using an MX/GNPs nanocomposite integrated with a low-power electronics module [64]. The MX/GNP hybrid served as the electrode interface and enabled the sensitive detection of dopamine and uric acid and was later extended to quantify cystatin C in human serum. For cystatin C, which is not intrinsically electroactive like dopamine and uric acid, the detection relies on an indirect electrochemical immunoassay format: binding of cystatin C to a specific recognition element on the MX/GNP surface modulates the interfacial impedance and accessibility of a redox probe. The consequent changes in DPV currents correlate quantitatively with cystatin C concentration. Thus, the mechanism combines direct electrocatalytic oxidation for small redox-active analytes and biorecognition-induced signal modulation for a protein biomarker, all transduced through the highly conductive, high-surface-area MX/GNP hybrid interface. Furthermore, clinical validation using samples from patients with gestational diabetes mellitus confirmed elevated cystatin C levels, demonstrating the system's

real-world diagnostic capability. The key materials contribution lies in the MX/GNP hybrid electrode, which combines high conductivity, large surface loading capacity, and compatibility with portable POC electronics.

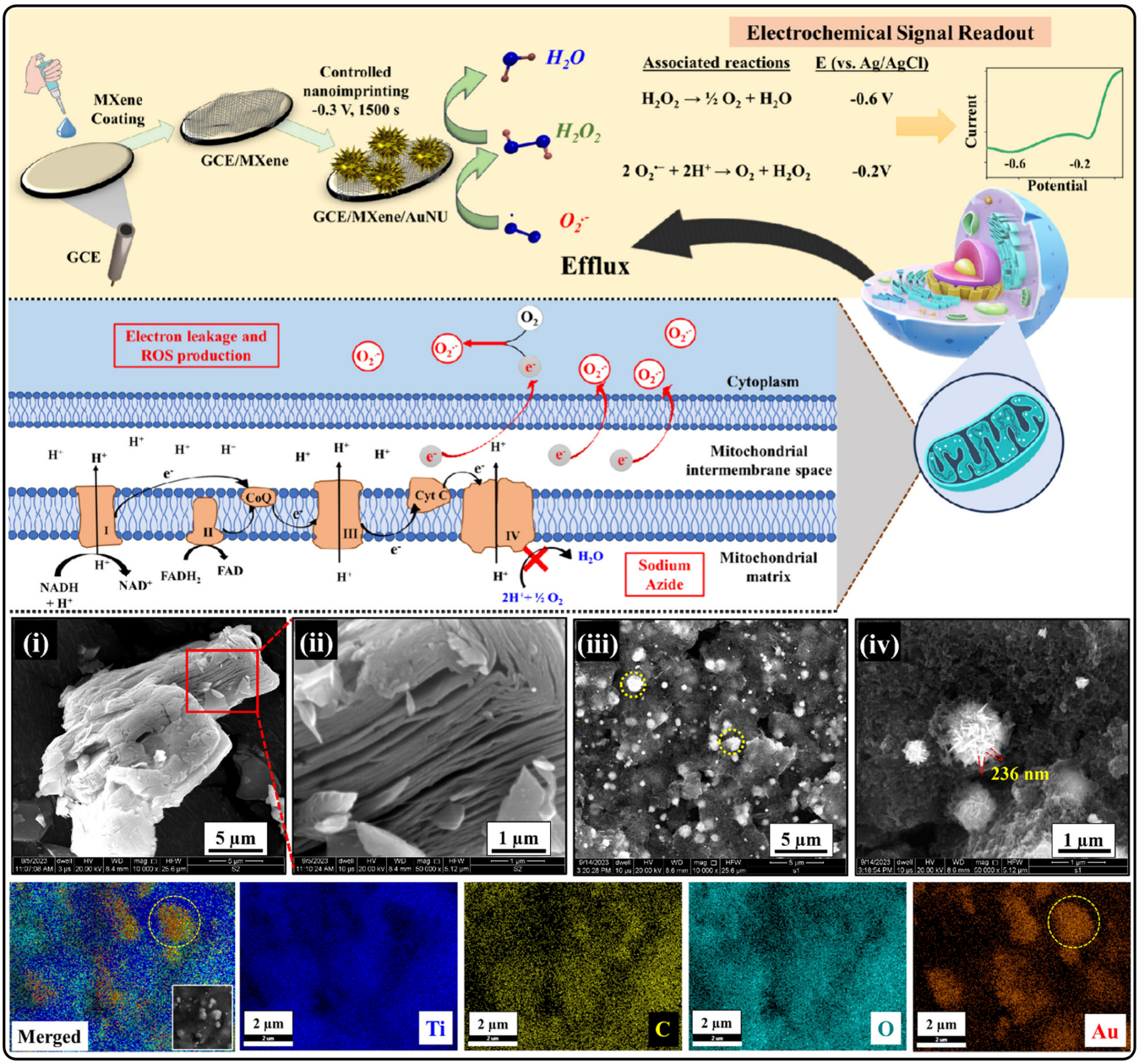

Figure 3. Graphical illustration of the fabrication of AuNu/MX/GCE sensor and its electrochemical sensing mechanism (electrochemical half-cell reactions) for detecting superoxide anions released from living cells. Inset shows the voltammetric response obtained for the reduction in superoxide anion radical (−0.2 V) and the subsequently formed hydrogen peroxide (−0.6 V). SEM images of (**i**,**ii**) MX nanosheets, (**iii**,**iv**) AuNu decorated MX nanosheets and their corresponding elemental mapping. Reproduced with permission from [58].

A flexible sensing electrode was fabricated by integrating a 3D laser-scribed graphene (LSG) scaffold with 2D MX nanosheets via a covalent C-O-Ti linkage, thereby forming a robust LSG-MX hybrid [65]. Subsequently, Au-Pd bimetallic NPs were deposited onto the hybrid via a room-temperature self-reduction process, producing shape-controlled Au-Pd nanostructures uniformly anchored on the LSG/MX surface. This material architecture integrates the high conductivity of graphene and MX, the large effective surface area of

the 3D–2D hybrid scaffold, and the abundant catalytic sites provided by the Au–Pd NPs. The composite electrode enabled simultaneous electrochemical detection of ascorbic acid, dopamine, and uric acid. Overall, this work demonstrates that combining 3D graphene, 2D MX, and self-reduced noble-metal bimetallic NPs yields a flexible, high-performance multi-analyte sensor platform. A hydrogen peroxide (H_2O_2) sensor platform was fabricated using 2D MX nanosheets functionalized with PtNPs, in which MX provides a high surface area, conductive layered scaffold with surface terminations (-O, -OH, -F) that facilitate nanoparticle anchoring, while PtNPs boost catalytic activity and electron-transfer kinetics [66]. Indeed, reports using Prussian blue as a redox-active mediator for H_2O_2 sensing highlight how catalytic layers can lower detection potentials and improve sensitivity [67], and this design principle is elegantly employed in this work, where MX is combined with PtNPs to yield a highly stable, low-potential H_2O_2 sensor. The resulting MX/PtNPs hybrid exhibited significantly improved redox stability, faster electron-transfer rates, and a reduced onset potential for H_2O_2 reduction compared with pristine MX. The key materials innovation lies in the integration of MX with noble-metal NPs, enabling a synergistic combination of high conductivity, abundant catalytic sites, and enhanced electrochemical stability for small-molecule sensing. In another study, a sustainable, flexible electrochemical sensor was fabricated by converting biopolymeric bacterial cellulose (BC) into an LSG network, followed by modification with 2D MX nanosheets and PtNPs [68]. BC, a renewable and biodegradable scaffold, transforms under laser irradiation into a conductive, graphene-like porous carbon network with high surface area and mechanical flexibility. Subsequent MX incorporation provides improved conductivity and enriched anchoring sites, while PtNPs serve as highly active electrocatalysts for H_2O_2 oxidation. The resulting BC-LSG/MX/PtNP electrode was successfully applied for monitoring H_2O_2 released from cancer cell models. This work highlights a green-fabrication route that merges biopolymer conversion, 2D materials, and noble-metal catalysis to create efficient biosensing platforms. A hollow, porous octahedral PtCu bimetallic nanocage was also synthesized using a Cu_2O sacrificial template and subsequently assembled onto 2D MX nanosheets via APTES-mediated electrostatic interactions [69]. The PtCu nanocages provide a high surface area, accessible internal porosity, and abundant catalytic sites, while the MX substrate offers a highly conductive support that accelerates charge transfer. The synergistic integration of hollow bimetallic nanocages with a 2D MX scaffold produced outstanding electrocatalytic performance for detecting endocrine-disrupting pollutants in water. This material design exemplifies how combining a hollow bimetallic catalyst with a conductive MX framework can markedly enhance electrocatalytic kinetics, active-site accessibility, and overall sensing efficiency for hazardous environmental analytes.

In another study, a nonenzymatic glucose sensor interface was engineered by electrochemically depositing Ni nanostructures onto MX sheets to form an MX/Ni hybrid [70]. The electrochemical deposition process enables intimate coupling between Ni and the MX surface, reducing charge-transfer resistance and enhancing interfacial electron mobility. The resulting sensor was applied for nonenzymatic glucose detection in saliva, demonstrating high sensitivity, strong stability, and good biocompatibility in a real biological fluid. This material architecture follows a "2D conductive support + transition-metal catalyst" design paradigm, consistent with current trends in enzyme-free electrochemical sensing. Another hybrid sensing interface was developed using 2D Nb-MX nanosheets decorated with selenium NPs (SeNPs). The composite was applied to modify a gold disc electrode and tested in an alkaline medium, demonstrating nonenzymatic glucose quantification [71]. The intimate MX/SeNPs interaction enhanced electron-transfer kinetics and stabilized the NPs against aggregation, thereby improving long-term sensor reliability. A hybrid 3D nanocomposite was designed for a wearable, patch-type electrochemical sensor. The core sensing layer

integrates Pt-decorated MX with nanoporous carbon, all embedded within a 3D graphene network [72]. The MX@Pt provides excellent catalytic activity and high conductivity from the metallic MX. The nanoporous carbon reinforces the structure, increasing surface area and porosity, thereby facilitating analyte access and mass transport. The 3D graphene scaffold gives mechanical robustness, flexibility, and a continuous electron-conductive network. Together, these components synergize: high catalytic sites (Pt), fast electron pathways (MX + graphene), and a porous architecture (nanoporous carbon) enabling sensitive, stable, and flexible sweat sensing across multiple analytes. In another study, to enhance the composite's electrochemical performance, PtNPs were incorporated into a hybrid framework consisting of SWCNTs, Ti-MX, and reduced graphene oxide (RGO), forming a highly conductive, high surface-area 3D network [73]. In this architecture, SWCNTs provide rapid electron-transport pathways and a large surface area for uniform PtNPs dispersion; MX contributes abundant surface functional groups and metallic conductivity; and RGO improves structural stability and facilitates synergistic electron transfer. The resulting composite exhibited well-resolved redox peaks, ultralow detection limits, and excellent reproducibility. Compared with conventional carbon- or metal-based sensing platforms, this multi-component hybrid demonstrates superior electrocatalytic activity and selectivity arising from the combined effects of nanoscale Pt catalysis, MX's functionalized conductive surfaces, and the CNT/RGO electron-transport "highways."

Across the reviewed studies, an explicit materials trend emerges for high-performance electrochemical sensing: 2D conductive scaffolds such as Ti- or Nb-MXs, graphene derivatives, or laser-scribed biopolymer networks are combined with catalytic NPs, including GNPs, PtNPs, SeNPs, bimetallic hybrids, and Au@COF-based hybrids to create interfaces that enhance electron transfer, surface area, and active site density. GNPs demonstrate remarkable versatility, serving both as signal amplification tags in biosensors and as electrocatalysts when coupled with MXs, thereby contributing to their widespread use across an increasing number of studies. Meanwhile, Pt, Ni, and Se NPs are increasingly being explored to expand the sensing range, target analytes, and substrate flexibility (rigid, flexible, or biopolymer-derived). The electrochemical performances of various MX-nanomaterial hybrids are compared in Table 2. Overall, these works collectively illustrate that hybrid 2D scaffold-nanoparticle architectures are now a dominant strategy in enzymeless, ultrasensitive, and real-matrix electrochemical sensors, with ongoing research focusing on sustainable scaffolds, diverse nanoparticle catalysts, and multiplexed applications.

Table 2. Electrochemical performances of various MX-nanomaterial based hybrids.

Sensor	Analyte	Linear Range (μM)	LOD (μM)	Sensitivity	Real Sample	Ref.
GNPs-Nb-MX	Progesterone	5.0×10^{-5}–1.6×10^{-4}	1.4×10^{-5}	1.59×10^{-7} μA pM^{-1}	Female sweat	[56]
MX/Au/GOx/SPCE	Glucose	0–200	13	0.33 μA μM^{-1} cm^{-2}	Human sweat	[57]
Ti-MX/GNU/GCE	Superoxide anions	1×10^{-4}–50	5.6×10^{-5}	-	Live cells	[58]
Ti-MX/GNPs/SPE	Cortisol	1.3×10^{-3}–1.379	* 100	-	Artificial sweat	[59]
Au-Ti-MX/Ab_1/CYFRA21-1/Ab_2-TB-Au-COF/GCE	Cytokeratin fragment antigen	* 0.5–1.0×10^4	* 0.1	-	Human serum	[60]
Au-Ti-MX/Apt/TB-Au@COFs	Amyloid-beta oligomer	* 0.01–180	* 4.27×10^{-3}	-	Human serum	[61]

Table 2. *Cont.*

Sensor	Analyte	Linear Range (μM)	LOD (μM)	Sensitivity	Real Sample	Ref.
Au/Ti-MX	Cardiac troponin I	1×10^{-10}–1×10^{-6} 1×10^{-10}–5×10^{-7}	4×10^{-14} 1×10^{-10}	-	Human serum	[62]
Ti-MX/Au/SPE	Fumonisin B1 Ampicillin	* 10–1×10^{6} 1×10^{-5}–0.5	* 1.617 2.2×10^{-16}	-	Corn, Wheat Tap water, Skim milk	[63]
Ti-MX/GNPs/SPE	Dopamine Uric acid Cystatin C	0–500 0–1000 * 5×10^{4}–5×10^{6}	1.11 1.12 -	118.280 nA μM^{-1} 52.975 nA μM^{-1} -	Pregnant women's serum samples	[64]
Au-Pd/MX/LSG/PI	Ascorbic acid Dopamine Uric acid	10–1600 12–240 8–800	3 0.13 1.47	-	Urine samples	[65]
Ti-MX/PtNPs/GCE	H_2O_2 Ascorbic acid Acetaminophen Dopamine Uric acid	490–53.6×10^{4} 0–750 0–750 0–750 0–750	0.448 0.25 0.13 0.26 0.12	- 1.41 μA mM^{-1} 8.00 μA mM^{-1} 3.68 μA mM^{-1} 6.85 μA mM^{-1}	-	[66]
BC-LSG/MX-PtNPs	H_2O_2	15–95	0.35	-	-	[68]
PtCu-Ti-MX/GCE	4-Nonylphenol 4-Tert-octylphenol Bisphenol A 17β-Estradiol	8×10^{-4}–40 9×10^{-4}–55 4×10^{-4}–35 6×10^{-4}–50	3.20×10^{-4} 2.70×10^{-4} 1.20×10^{-4} 1.9×10^{-4}	-	Industrial sewage, breeding wastewater, lake & river water	[69]
Ni/Ti-MX/GCE	Glucose	1–7507	1	2.736×10^{5} μA μM^{-1} cm^{-2}	Saliva Blood	[70]
Au/SeNPs/Nb-MX/GCE	Glucose	2–3×10^{4}	1100	4.150×10^{3} μA μM^{-1} cm^{-2}	-	[71]
LIG/MX@Pt/PtNPs	Glucose	0–2000	3	8.645×10^{4} μA μM^{-1} cm^{-2}	Human sweat	[72]
Ti-MX/SWCNT/PtNPs	Bisphenol A Dimethyl bisphenol A	6×10^{-3}–7.4	2800 0.003	1.607 & 1.321 μA μM^{-1} cm^{-2}	Thermal paper	[73]

BC—bacterial cellulose; COF—covalent organic framework; CYFRA21-1—cytokeratin fragment antigen 21-1; GOx—glucose oxidase; GNPs—gold nanoparticles; GNU—gold nanourchins; LIG—laser induced graphene; LSG—laser-scribed graphene; PtNPs—platinum nanoparticles; SPCE—screen printed carbon electrode; SeNPs—selenium nanoparticles; TB—toluidine blue; *—pg mL^{-1}.

2.3. MXene–Metal Oxide Hybrids

Metal oxides are widely recognized for their excellent catalytic activity, chemical stability, and diverse redox behavior, making them valuable materials for applications in energy conversion, storage, and sensing applications [74]. However, their intrinsic low electrical conductivity and tendency to aggregate often restrict their electrochemical efficacy [75]. When integrated with highly conductive and hydrophilic MX, these limitations can be effectively mitigated. The incorporation of MX sheets establishes a continuous electron-transport network, significantly enhancing the hybrid's conductivity and enabling rapid charge transfer during redox processes. Simultaneously, the metal oxides contribute abundant electroactive sites and strong catalytic activity, while also helping to prevent MX restacking and improving its structural stability against oxidation. This synergistic coupling between MX and metal oxides enhances both electronic and ionic transport, increases the utilization of active surface area, and reinforces overall structural robustness. As a result,

MX–metal oxide hybrids demonstrate superior electrochemical performance, successfully combining the high catalytic activity of metal oxides with the exceptional conductivity, flexibility, and processability of MX [76]. This integrated architecture is particularly advantageous for developing high-performance electrochemical sensors. The following section highlights recent studies on MX–metal oxide hybrid systems and their applications in various aspects of electrochemical health monitoring.

An electrochemical aptasensor was constructed using an MX-Fe_2O_3 hybrid for the ultrasensitive detection of testosterone [77]. Testosterone is a key androgen involved in numerous physiological processes, including muscle mass regulation, bone density maintenance, sexual function, and mood modulation. Abnormal testosterone levels are associated with conditions such as hypogonadism, polycystic ovary syndrome, cardiovascular risk, and other endocrine disorders, making its accurate monitoring essential for clinical assessment. In this work, Fe_2O_3 NPs were integrated with MX sheets to form a hybrid with enhanced surface area, improved conductivity, and increased capacity for aptamer immobilization. MX provided a highly conductive layered scaffold, while Fe_2O_3 offered abundant redox-active catalytic sites and facilitated strong aptamer attachment. This hybridization strategy exploited the synergy between the conductive MX framework and the catalytic properties of the metal oxide, resulting in a binder-free material with high interfacial contact and without the aggregation or contact-resistance issues typically observed in pure metal oxide based sensors. The MX-Fe_2O_3 hybrid exhibited excellent electrical conductivity, robust mechanical stability, a large electroactive surface area, and a favorable interface for aptamer functionalization. The aptasensor achieved an ultralow detection limit, high selectivity against structurally similar hormones, and reliable performance in real water samples, demonstrating both high analytical sensitivity and strong practical applicability. A similar hybrid nanomaterial comprising magnetic Fe_3O_4 integrated MX sheets was synthesized for electrochemical sensing of the anticancer drug idarubicin [78]. Idarubicin is widely used in chemotherapy but is associated with dose-dependent cardiotoxicity and hematological side effects, making its sensitive and accurate monitoring in biological matrices clinically important. In this work, Fe_3O_4 NPs were anchored onto MX sheets to form a conductive, magnetically active hybrid scaffold in which the magnetite provides catalytic activity and MX offers high conductivity and a large accessible surface area. The close interfacial contact between MX and Fe_3O_4 enhanced electron-transfer kinetics, prevented MX restacking, and enabled magnetic enrichment of the analyte, collectively improving sensitivity and electrocatalytic performance toward idarubicin detection.

A $FeVO_4$ nanoflake-decorated MX hybrid was developed as a novel electrochemical biosensor for the detection of serotonin [79]. Serotonin plays essential roles in mood regulation and various physiological functions, and its dysregulation is associated with depression, cardiovascular disorders, and other neurological conditions, making its accurate monitoring clinically important. The $FeVO_4$@MX hybrid was synthesized by growing $FeVO_4$ nanoflakes directly on MX sheets, producing a 2D conductive network enriched with numerous catalytically active sites. This hierarchical architecture enhanced electron-transfer efficiency, prevented MX restacking, and improved overall structural stability. Compared with the previously reported MX/Fe_2O_3 testosterone sensor, this sensor exhibited superior interfacial contact and stronger redox activity, contributing to improved electrocatalytic performance toward serotonin. A hybrid sensor built from single-layer MX sheets and electrospun 1D $FeWO_4$ nanofibers was fabricated for the ultrasensitive detection of the flavonoid rutin [80]. Rutin is a naturally occurring antioxidant found in various plants and foods and is associated with multiple health benefits, including anti-inflammatory activity and vascular protection; however, its sensitive quantification is essential for dietary, nutritional, and pharmaceutical monitoring. The heterostructure was synthesized by elec-

trospinning $FeWO_4$ nanofibers and subsequently anchoring them onto delaminated MX sheets, forming an interlinked 2D-1D conductive network. This architecture offers several advantages, including a large interfacial contact area, abundant defects and catalytic sites, prevention of MX restacking, and enhanced catalytic activity arising from the metal oxide component. The sensor exhibited excellent stability, reproducibility, anti-interference capability, and reliable recovery in real sample analyses. Compared with previously reported MX/metal-oxide systems, this work highlights the benefits of a 2D-1D hybrid structure and demonstrates its effectiveness for detecting a bioflavonoid analyte rather than a hormone, achieving similarly high analytical performance.

A wearable sensing platform was developed for lactate monitoring using a carbonized rice-paper substrate combined with a few-layer MX and ZIF-67-derived microcubes [81]. Lactate is an important sweat biomarker that reflects muscle activation and fatigue; elevated levels in sweat or blood may indicate strenuous exercise, metabolic imbalance, sepsis, or hypoxia. In this work, rice paper was carbonized to form a flexible, porous, and conductive substrate, followed by layer-by-layer assembly of MX and ZIF-67 microcubes. Pyrolysis was then used to convert ZIF-67 into its corresponding metal-oxide composite. This fabrication strategy provides a flexible, binder-free electrode with strong mechanical integrity, a large surface area, intimate MX-metal oxide contact, and excellent scalability. The resulting hybrid exhibited high electrical conductivity, a highly porous microstructure, strong adhesion, and good flexibility, and these properties are well-suited for wearable and implantable devices. As a sensor, it showed high sensitivity toward lactate in sweat, strong anti-interference capability, good stability, and seamless compatibility with wearable form factors. In another work, an MX/$MnCo_2O_4$ hybrid was developed for the electrochemical detection of the environmental pollutant p-nitrotoluene (p-NT) [82], a toxic nitroaromatic compound known for its persistence and carcinogenic effects, making sensitive detection crucial for environmental and health monitoring. The hybrid was synthesized using a simple ultrasonic-assisted method that facilitated uniform dispersion of $MnCo_2O_4$ NPs across MX sheets, yielding enhanced conductivity, abundant catalytic sites, and strong interfacial coupling. The sensor delivered a wide linear range, high sensitivity, and excellent stability. Compared with the rice-paper lactate sensor, this work focuses on environmental applications and employs a simpler synthesis while achieving superior electron-transfer performance. In a similar way, a nonenzymatic sweat glucose sensor was developed using $NiCo_2O_4$ NPs anchored onto double-MX sheets (Ti-Nb-MX) [83]. The $NiCo_2O_4$/Ti-Nb-MX hybrid was synthesized via an in situ growth approach, ensuring strong interfacial contact, high conductivity, and abundant catalytic sites. The sensor exhibited excellent electrocatalytic activity, high sensitivity, and stable performance in human sweat samples. This study highlights a biocompatible and robust design for wearable glucose monitoring using a double-MX framework.

A creatinine sensor was developed using a hybrid material composed of lanthanum-doped nickel-cobalt ferrite NPs grown on few-layer MX (La@$NiCoFe_2O_4$@Ti-MX), which was synthesized via a hydrothermal route [84]. In another study, a 1D-2D $MnMoO_4$-MX nanohybrid was engineered for the simultaneous electrochemical detection of hydroquinone and catechol, two highly toxic dihydroxybenzene isomers that pose significant environmental and public-health risks [85]. The hybrid was prepared by integrating electrospun $MnMoO_4$ nanofibers with exfoliated MX sheets, creating a porous, high surface area network with strong interfacial coupling that enhances charge transport and catalytic activity. This structural synergy facilitates efficient redox reactions and enables reliable discrimination between the coexisting pollutants. Compared with previous MX-metal oxide hybrids, this work highlights an environmental-sensing direction and demonstrates

that 1D-2D architectures can deliver superior selectivity and electron-transfer efficiency across diverse analyte systems.

Similarly, a 2D sheet-structure hybrid consisting of $ZnMoO_4$ nanoflakes decorated onto MX sheets was developed for the selective electrochemical detection of the arsenic-based veterinary drug roxarsone in water [86]. Roxarsone is considered hazardous due to its arsenic content, persistence, and mobility in aquatic environments, making its sensitive detection essential for environmental safety. In this work, $ZnMoO_4$ nanoflakes were anchored onto the MX scaffold, producing a 2D-2D hybrid with enhanced electron-transfer pathways and a high density of catalytic active sites. Unlike previous studies focused on biological analytes, this work targets an arsenic-containing pharmaceutical pollutant and employs a purely 2D-2D hybrid architecture rather than mixed dimensionality. The sensor demonstrated strong selectivity, excellent analytical performance, and practical recoveries in real water samples, highlighting its effectiveness for environmental monitoring.

A hybrid sensor material composed of samarium oxide (Sm_2O_3) flakes grown on 2D Ti-MX through a facile hydrothermal process was developed for the detection of the antihypertensive drug nimodipine in biological samples [87]. Sm_2O_3 provides abundant redox-active sites, while the Ti-MX backbone ensures high conductivity and efficient ion transport, together yielding a sensor with excellent selectivity, stability, and repeatability in complex biological matrices. Compared with earlier MX-metal oxide systems, this study is distinguished by the use of a rare-earth oxide/MX hybrid for drug detection, demonstrating the broad adaptability of MX–metal oxide architectures across various sensing domains. A biosensor was also constructed using Eu^{3+}-doped SnO_2 NPs embedded within exfoliated MX laminates to form a hybrid matrix for enzymatic electrochemical lactate sensing [88]. This design exploits the high catalytic reactivity of Eu-SnO_2 and the superior conductivity and layered structure of MX, enabling rapid electron transport and an efficient enzyme–electrode interface. In contrast to previous nonenzymatic MX-metal oxide sensors, this work uniquely integrates metal-oxide doping with enzymatic recognition on an MX scaffold, emphasizing enhanced biochemical compatibility and interface engineering for improved analytical performance.

A novel MX composite infused with Co_3O_4 NPs was engineered as a high-performance sensing interface for the detection of 4-aminophenol [89]. The material was constructed by exfoliating Ti-MX sheets, decorating them with Co_3O_4 NPs, and embedding the resulting hybrid into electrospun carbon nanofibers (CNFs), which serve as a porous, conductive, and mechanically stable scaffold. In this architecture, MX provides rapid electron transport and abundant surface functional groups, contributes strong redox-mediated electrocatalytic activity, and the CNFs prevent nanoparticle aggregation while maintaining structural integrity. Rather than acting as isolated components, these units form a synergistic, interconnected network that significantly increases the electroactive surface area, reduces charge-transfer resistance, and enhances long-term stability. This study demonstrates that combining a 2D conductor, a transition-metal-oxide catalyst, and a carbon-fiber framework creates a highly efficient and durable electrochemical platform, offering an alternative design pathway to the CNT- and graphene-based hybrid systems typically used in current electrochemical sensor development. In another study, a quaternary nanohybrid composed of MX, MWCNT, GNPs, and Fe_3O_4 was engineered to construct a high-efficiency choline biosensing interface, where each component contributes a distinct yet synergistic function toward optimized signal transduction [90]. MX serves as a highly conductive 2D scaffold with abundant surface terminations, but its intrinsic tendency to restack is effectively mitigated by the incorporation of MWCNT–GNP structures; the tubular morphology of MWCNTs prevents layer collapse, while the attached GNPs enhance catalytic activity and facilitate rapid electron shuttling. Fe_3O_4, NPs further introduce peroxidase-like catalytic

behavior and magnetic properties, which improve mass transport and significantly reduce sensor response time. Upon integration with immobilized choline oxidase, these components form an interconnected, high-conductivity network that increases enzyme loading capacity, lowers charge-transfer resistance, and expands the effective electroactive surface area. This work demonstrates that layering 2D MX sheets with CNT-based conductive pathways and catalytically active Fe_3O_4 provides a powerful strategy to overcome the individual limitations of each material, yielding a robust and highly responsive biosensing platform.

A highly engineered ternary hybrid material was developed by integrating NiO NPs, RGO, and MoTi-MX, with each component contributing complementary structural and functional advantages [91]. MoTi-MX, obtained through etching and subsequent delamination, provides a conductive layered 2D framework with expanded interlayer spacing that facilitates efficient electron and ion transport. The RGO synthesized from industrial graphite waste and chemically reduced with hydrazine acts as a high surface-area, defect-rich, conductive carbon network that prevents MX sheet restacking and enhances overall material stability. NiO NPs, formed in situ and uniformly anchored onto the RGO sheets, introduce abundant redox-active Ni^{2+}/Ni^{3+} sites. The resulting structural synergy enhances electron-transport pathways, increases ion-accessible surface area, optimizes pore distribution, and strengthens interfacial interactions.

Collectively, the reviewed studies underscore the exceptional versatility of MX–metal oxide hybrid architectures across biomedical, pharmaceutical, and environmental electrochemical sensing applications. By tuning dimensionality (1D/2D/3D), metal oxide composition, and synthesis strategy, these hybrids achieve tailored conductivity, active-site density, and structural robustness suited to specific analyte requirements. Biomedical sensors—such as MX/ZIF-67 for lactate, $NiCo_2O_4$/double-MX for glucose, and La@$NiCoFe_2O_4$ for creatinine- emphasize flexibility, biocompatibility, and nonenzymatic operation for wearable biosensing. In contrast, environmental sensors like MX/$MnCo_2O_4$ for p-NT, MnMoO4/MX for dihydroxybenzenes, and $ZnMoO_4$/MX for roxarsone prioritize catalytic efficiency and selective detection of persistent pollutants. Drug detection systems such as Sm_2O_3/Ti-MX for nimodipine highlight the adaptability of MX hybrids for complex biological matrices, while enzymatic platforms like Eu-SnO_2/MX demonstrate improved redox behavior and enhanced enzyme–electrode interfacing. The electroanalytical performances of various MX-metal oxide hybrids are given in Table 3. Overall, these works show that MX–metal oxide hybrids, through deliberate compositional and structural modulation, produce synergistic enhancements in conductivity, catalytic activity, and interfacial stability, enabling high sensitivity, strong selectivity, and excellent operational stability across a diverse range of electrochemical sensing applications.

Table 3. Electrochemical performance comparisons of various MX-metal oxide hybrids.

Sensor	Analyte	Linear Range (μM)	LOD (μM)	Sensitivity	Real Sample	Ref.
Ti-MX/Fe_2O_3	Testosterone	* 0.4–50	* 1.5×10^{-3}	-	Water	[77]
MX/Fe_3O_4	Idarubicin	0.1–4	2.643×10^{-2}	-	Human, plasma, urine	[78]
Ti-MX/$FeVO_4$	Serotonin	2.5×10^{-2}–7.5×10^{-1}	5.88×10^{-3}	3.0 μA μM^{-1} cm^{-2}	Human serum	[79]
MX/$FeWO_4$	Rutin	4×10^{-3}–1.47×10^{-1}	4.2×10^{-4}	379.9 μA μM^{-1} cm^{-2}	Human serum, orange juice, black tea	[80]

Table 3. *Cont.*

Sensor	Analyte	Linear Range (μM)	LOD (μM)	Sensitivity	Real Sample	Ref.
Ti-MX/CoO/ZIF-67	Lactate	10–360	3.2	-	Human sweat	[81]
Ti-MX/$MnCo_2O_4$	p-nitrotoluene	0.18–4170	3.51×10^{-2}	1.71 μA μM^{-1} cm^{-2}	Pond water, tap water	[82]
TiNb-MX/$NiCo_2O_4$	Glucose	-	298	4.256×10^5 μA μM^{-1} cm^{-2}	Blood, sweat	[83]
Ti-MX/$NiCoFe_2O_4$/La	Creatinine	0–1000	-	-	-	[84]
MX/$MnMoO_4$	Hydroquinone Catechol	5×10^{-3}–6.5×10^{-2}	2.6×10^{-4} 3.0×10^{-4}	7437 & 6471 μA μM^{-1} cm^{-2}	River water, sea water	[85]
MX/$ZnMoO_4$	Roxarsone	50–300	0.008	10.413 μA μM^{-1} cm^{-2}	Tap water, drinking water, river water, pond water	[86]
TiC/Sm_2O_3	Nimodipine	50–675	4.2×10^{-3}	1.5 μA μM^{-1} cm^{-2}	Human urine and blood serum	[87]
Ti-MX/Eu-SnO_2/Lox	Lactate	1×10^{-3}–100	3.38×10^{-4}	4.815×10^6 μA μM^{-1} cm^{-2}	Human serum	[88]
Ti-MX/Co_3O_4/CNF	4-aminophenol	0.5–150	0.018 μM	-	Tap water, blood serum	[89]
MX/MWCNT/GNP/Fe_3O_4	Choline	0.033–133.33	2.2×10^{-2}	8.8×10^{-3} μA μM^{-1} cm^{-2}	Human serum, CSF	[90]
MoTi-MX/RGO/NiO	Dopamine	0.002–0.012	1.44×10^{-3}	1.441×10^{-4} μA μM^{-1}	Human urine and serum	[91]

CSF—cerebrospinal fluid; GNP—gold nanoparticle; MWCNT—multiwalled carbon nanotube; RGO—reduced graphene oxide; *—ng mL^{-1}.

2.4. MXene with Metal–Organic Framework Hybrids

Metal–organic frameworks (MOFs) are highly crystalline porous materials formed through coordination bonding between metal nodes and organic linkers. They exhibit large surface areas, tunable porosity, extensive synthetic and chemical versatility, moderate to good electrical conductivity, and excellent electrocatalytic activity [92]. The integration of MOFs with MX has recently emerged as a promising research direction, as such hybrids aim to enhance the intrinsic conductivity and structural stability of MOFs while simultaneously preventing MX interlayer restacking and improving catalytic performance toward various important analytes [93]. The following section summarizes recent advances in MX-MOF based electrochemical sensors, highlighting the significance of these hybrid architectures, their preparation methodologies, and their electrocatalytic activities toward biologically and environmentally relevant analytes.

Roy and colleagues developed a POC sensor for blood creatinine detection using cobalt MOF decorated MX nanosheets [94]. Creatinine is a metabolic byproduct filtered by the kidneys and excreted through urine, and its selective detection is crucial since its concentration in blood serves as an important indicator of kidney function and related disorders. In this work, Ti_3C_2 MX nanosheets were first synthesized, and Co MOF structures were subsequently grown in situ on their surface. The resulting hybrid was then mixed with carbon black (CB) in a 1:10 ratio and printed onto a substrate. In this configuration, CB acted as a binder and carrier medium, facilitating the uniform distribution of the nanohybrid, while the Co MOF served as a nanofiller and electrocatalyst for creatinine detection. The sensor performance was validated through the quantification of creatinine in human serum samples, demonstrating excellent selectivity, stability and reproducibility. Similarly,

a 3D@2D nanohybrid was developed for the selective detection of dopamine using ZIF-67 embedded within 2D MX nanosheets [95]. Dopamine is an excitatory neurotransmitter that plays critical roles in the central nervous system, including the regulation of motor function, cardiovascular activity, gastrointestinal processes, and cognitive behavior. It also serves as an important biomarker for neurodegenerative disorders. In this work, 3D ZIF-67 structures were grown in situ on titanium carbide MX sheets, and the resulting hybrid ink was coated onto a GCE to fabricate the dopamine sensor. The formation of the 3D@2D hybrid significantly enhanced the number of active surface sites, electrocatalytic activity, and electron-transfer kinetics, leading to improved dopamine-sensing performance. In another study, a bimetallic MOF-decorated MX nanohybrid was utilized for the detection of the antibiotic chloramphenicol [96]. Chloramphenicol is a widely used broad-spectrum antimicrobial agent; however, its persistence in biological and environmental systems can lead to severe adverse effects, including leukopenia, anemia, bone-marrow suppression, and gray baby syndrome. Therefore, its selective and sensitive quantification is crucial for ensuring human health. Here, MX nanosheets were in situ decorated with CoFe-MOF nanostructures and deposited onto hydrophobic carbon paper to construct the sensor. This hybrid architecture enhanced adsorption capability and significantly improved electrocatalytic activity toward chloramphenicol detection.

Richard and coworkers developed a bio-MOF embedded MX nanohybrid for the real-time monitoring of melatonin, an essential sleep hormone [97]. Melatonin plays a vital role in regulating circadian rhythms, learning, dreaming, immune function, fertility, and reproductive health; therefore, its precise quantification is clinically important. In their work, a Zn-based bio-MOF was synthesized from L-glutamic acid, while niobium carbide MX was prepared from niobium aluminum carbide. The two components were then ultrasonically mixed in different proportions to form the hybrid sensing material, as shown in Figure 4. The resulting nanohybrid exhibited enhanced electrocatalytic activity, an increased density of catalytically active sites, and improved sensitivity and selectivity toward melatonin. The synergistic interaction between MX and the MOF significantly strengthened the overall electrochemical performance. Another Zn-MOF embedded in Ti-MX hybrid was developed as a host-guest sensor for the selective sensing of dopamine [98]. In this case, an amine-terminated Zn MOF was synthesized and ultrasonically anchored onto the MX nanosheets to form the sensing interface. For comparison, in situ MOF/MX hybrids were also prepared; however, these showed inferior activity compared to the post-synthetically assembled hybrid. This improvement was attributed to the greater availability of free terminal amine groups in the post-synthetic product, which promoted stronger nonspecific interactions with dopamine and facilitated more efficient preconcentration. Consequently, the post-synthetic MOF/MX hybrid demonstrated superior electrocatalytic performance. In another study, an aptasensor for zearalenone detection was constructed using a titanium MOF decorated Ti-MX [99]. Zearalenone is an estrogenic mycotoxin produced by *Fusarium graminearum* and is commonly present in cereals such as sorghum, wheat, and corn, where it poses risks including immunotoxicity, hepatotoxicity, and reproductive toxicity. In this work, MX sheets were first synthesized and subsequently embedded in situ with amine-terminated titanium MOF (MIL-125). The resulting composite was covalently coupled with polyethyleneimine (PEI) to produce the aptasensor. Incorporation of the MOF not only enhanced electrocatalytic activity but also increased the number of available binding sites for aptamer immobilization, thereby improving overall sensing performance.

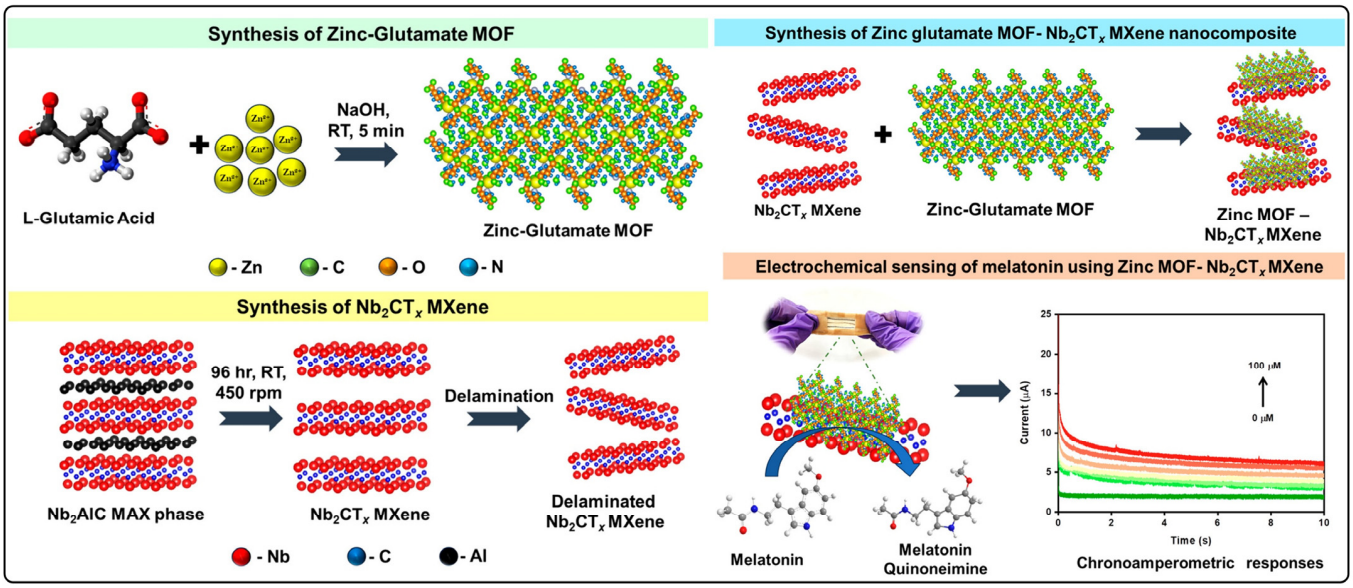

Figure 4. Graphical representation of the stepwise synthesis of glutamate-Zn MOF incorporated Nb-MX nanohybrid and its electrocatalytic activity toward melatonin. Reproduced with permission from [97].

A molybdenum MOF decorated titanium carbide MX nanohybrid was developed for the selective detection of aflatoxin B1 [100]. Aflatoxin B1 is a highly toxic secondary metabolite produced by several fungal species and is known to exhibit mutagenic, teratogenic, and carcinogenic effects, making its routine monitoring critically important. Here, amine-functionalized Mo-MOF was synthesized and then ultrasonically deposited onto titanium carbide MX to form the hybrid. This hybrid was subsequently covalently coupled with aflatoxin antibodies to construct the proposed biosensor. In another study, Ti-MX nanosheets were decorated with in situ grown Zr-MOF and employed for the sensitive detection of acetaminophen [101]. Acetaminophen is a widely used antipyretic and analgesic drug available over the counter; however, consumption above the recommended dose can lead to serious adverse effects, including nausea, vomiting, renal damage, and liver failure [102]. A ternary composite was engineered through a sequential hydrothermal-electrostatic assembly of MX/MOF/PtNPs to overcome two major material bottlenecks of MX restacking and the intrinsically poor conductivity of MOFs [103]. In this design, hydrothermally grown MOF nanostructures intercalated uniformly between Ti-MX layers, physically spacing the sheets apart and suppressing van der Waals-driven restacking, which in turn significantly enhanced electron mobility within the hybrid. Subsequently, PtNPs were electrostatically adsorbed onto the positively charged MX/MOF surface, increasing the electroactive surface area, accelerating ion transport, and serving as conductive bridges that electrically couple MOF nodes to the MX backbone. Following deposition of a sol–gel derived MIP, the composite acquired highly selective recognition cavities for diethylstilbestrol, which modulated electron-transfer pathways during sensing. Optimization of the MX:MOF ratio was critical, as it maximized conductivity by balancing adequate interlayer dispersion while avoiding excessive MOF content that could introduce resistive domains. This study exemplifies how hetero-interface design, MX 2D conductivity, MOF-derived structural dispersion, and Pt-mediated catalytic wiring can be orchestrated to surpass the performance limitations of conventional MX/MOF hybrids, providing a compelling template for next-generation selective sensing platforms across a wide range of analytical applications.

Overall, the incorporation of MOF nanostructures into MX nanosheets enhanced material stability, prevented MX layers from aggregating, improved the adsorption capa-

bility of the nanohybrids, augmented electrocatalytic activity, and increased the number of catalytically active sites. In addition, functionalized MOF nanostructures provided a stable microenvironment for the effective covalent immobilization of enzymes, aptamers, and antibodies, while their biocompatible nature helped preserve the native structure and activity of these biomolecules. Table 4 compares the electroanalytical performances of various MX-MOF hybrids.

Table 4. Electrochemical performance of different MX-MOF hybrids.

Sensor	Analyte	Linear Range (μM)	LOD (μM)	Sensitivity	Real Sample	Ref.
Co-MOF-Ti-MX@CB	Creatinine	10–800	5×10^{-3}	1.1 μA μM^{-1}	Human serum	[94]
ZIF-67@Ti-MX/GCE	Dopamine	0.05–100	1.7×10^{-2}	2.73 μA μM^{-1} cm^{-2}	Blood serum and injection solution	[95]
CoFe-MOF/Ti-MX/HCP	Chloramphenicol	1×10^{-4}–2×10^{-3}	3.3×10^{-5}	-	Water, milk and urine	[96]
Glu-Zn-MOF-Nb-MX	Melatonin	1–100	2.15×10^{-1}	-	Sweat, blood, serum and CSF	[97]
Zn-MOF/MX/GCE	Dopamine	1–6 × 10^3	0.0564	263.8 μA μM^{-1} cm^{-2}	Human serum	[98]
PEI@Ti-MOF/Ti-MX/AuE	Zearalenone	* 1×10^{-5} to 10	* 1.6×10^{-6}	-	Corn meal and beer	[99]
Mo-MOF/Ti-MX/SPE	Aflatoxin B1	* 0.06–50	* 8×10^{-3}	-	Pistachio	[100]
Zr-MOF-Ti-MX/GCE	Acetaminophen	0.032–160	0.01	1.235 μA μM^{-1} cm^{-2}	Water samples	[101]
MX/NH_2-UiO-66/PtNPs	Diethylstilbestrol	1×10^{-5}–1×10^2	1.1×10^{-6}	-	Tap water, Milk Chicken	[103]

AuE—gold electrode; CB—carbon black; CSF—cerebrospinal fluid; Glu—glutamate; HCP—hydrophobic carbon paper; PEI—polyethyleneimine; ZIF—zeolitic imidazolate framework; *—ng mL^{-1}.

2.5. MXene-Covalent Organic Framework Hybrids

Similar to MOFs, covalent organic frameworks (COFs) are porous crystalline materials with highly ordered structures. However, unlike MOFs, COFs are composed entirely of light elements such as C, H, N, O, and B, connected through strong covalent bonds. These organic building blocks self-assemble into 2D or 3D periodic architectures, forming frameworks with exceptional structural regularity and stability. COFs possess several attractive properties, including large surface area, tunable porosity, excellent synthetic versatility, and high chemical and thermal stability [104]. COFs have been widely explored in electrochemical sensing due to their intrinsic porosity, which facilitates molecular recognition, immobilization of biomolecules, and loading of electroactive species. Their tailorable functional groups support both chemical and physical attachment of diverse biorecognition units, while their robust and reusable nature enhances sensor longevity. COFs can also form hybrid nanostructures with other nanomaterials, often resulting in synergistic improvements in electrocatalytic activity [105]. Incorporating COFs into MX nanolayers offers several advantages: they act as interlayer spacers to prevent MX restacking, enhance surface functionality, and serve as protective barriers that mitigate oxidation or degradation of MX sheets. As a result, MX-COF hybrids exhibit improved structural stability, enhanced catalytic activity, and superior selectivity, making them promising candidates for advanced electrochemical sensing applications.

A COF-decorated niobium carbide MX (Nb-MX) hybrid was developed for the electrochemical sensing of epinephrine [106]. Epinephrine, a key hormone and neurotransmitter, is an important biomarker for stress monitoring and physiological regulation. Secreted by the adrenal medulla, it performs essential functions including increasing heart rate, regulating blood pressure, and inducing vasoconstriction. In this work, MX nanosheets were first synthesized independently, followed by the incorporation of COF nanostructures through a solvothermal process (Figure 5). The resulting hybrid exhibited excellent electrocatalytic activity toward epinephrine, achieving a detection limit of 1.09 μM and demonstrating good recovery values in urine and serum samples.

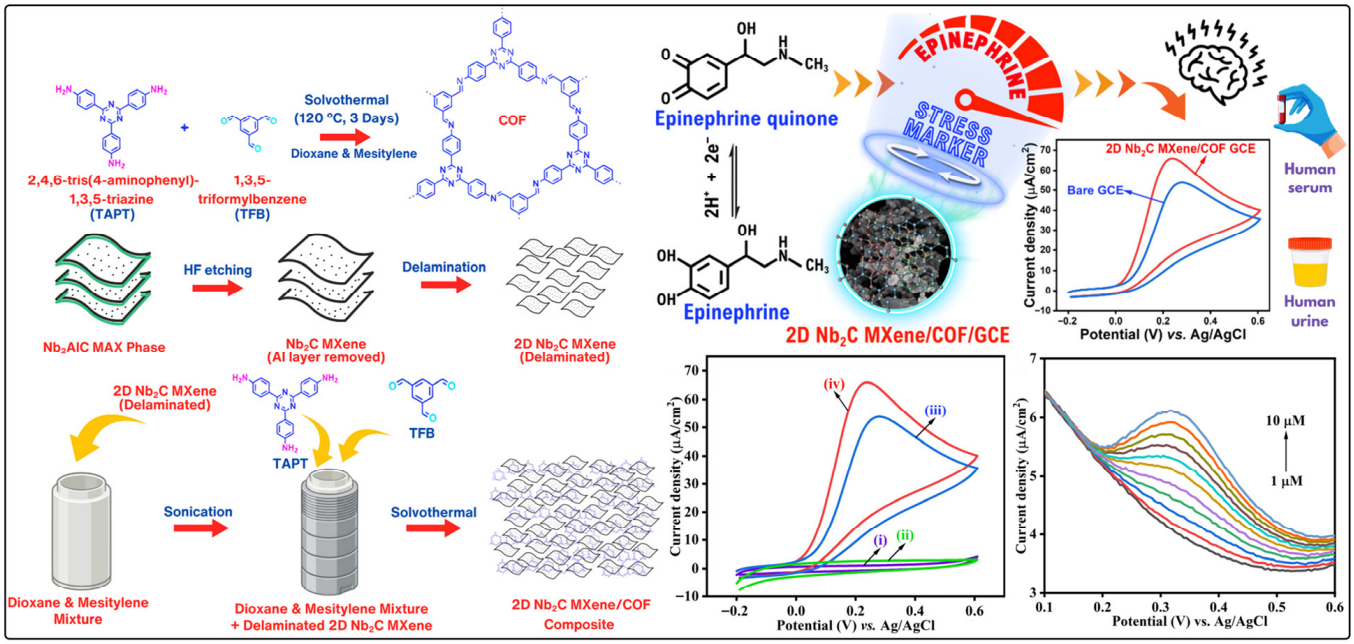

Figure 5. Schematic representation for the synthesis of MX-COF hybrid and its electrochemical response toward epinephrine detection, with potentials referenced to a standard Ag/AgCl reference electrode. Reproduced with permission from [106].

Similarly, a ratiometric electrochemical sensor was developed for the detection of dopamine using a β-ketoenamine COF-decorated MX hybrid [107]. The COF nanostructure was synthesized in situ on MX sheets using TFP (2,4,6-tris(4-formylphenyl)pyridine) and DAAQ (2,6-diaminoanthraquinone) as precursors. Incorporation of the COF enhanced the surface functionality of MX, enabling stronger and more selective interactions with dopamine through hydrogen bonding and van der Waals forces. As a result, the sensor showed excellent electrocatalytic performance, with a wide linear detection range of 0.05–800 μM and a detection limit of 6.1 nM. Its practical applicability was confirmed by the successful quantification of dopamine in human serum and pharmaceutical injection samples. In another study, a host-guest recognition based electrochemical sensor was developed for the detection of zearalenone in cereal products using a hybrid composed of MX, COF, GNPs and β-cyclodextrin (BCD) [108]. In this design, MX was first synthesized from its MAX precursor, followed by solvothermal growth of a triptycene based COF to form the MX-COF hybrid. This hybrid was then electrodeposited with GNPs and subsequently electropolymerized with BCD to yield the final sensing interface. The in situ self-assembly process enhanced structural stability and resulted in a twofold increase in the electrochemical response. The incorporation of BCD provided host-guest inclusion capability, enabling selective interaction with the target mycotoxin zearalenone. The sensor displayed a linear detection range of 0.04–0.5 μg mL^{-1} with a detection limit

of 0.01 μg mL^{-1} and demonstrated excellent recoveries in cereal samples. Similarly, an MX-COF hybrid was synthesized in situ and utilized for the simultaneous quantification of adenine and guanine [109]. Adenine and guanine are purine bases whose concentration variations reflect physiological status and metabolic function. However, selective electrochemical quantification is challenging due to their structurally similar characteristics. In this work, amine-functionalized MX nanosheets were first prepared, and COF nanostructures derived from TAPT and DHTA monomers were grown in situ to form a sandwiched MX-COF hybrid. This hierarchical structure enabled sensitive and selective detection of both analytes independently and simultaneously. The enhanced performance was attributed to the significant increase in specific surface area and the abundance of catalytically active sites, which together boosted electrocatalytic activity and sensitivity.

Overall, these studies demonstrate that integrating COFs with MX architectures significantly enhances structural stability, surface functionality, and electrocatalytic performance, underscoring the broad potential of MX-COF hybrids as versatile platforms for high-performance electrochemical sensing across diverse analyte classes.

2.6. MXenes Hybrids with Molecularly Imprinted Polymers

A nanohybrid sensor material was engineered by bridging 2D Ti-MX nanosheets with amino-functionalized MWCNTs using a thin polydopamine (PDA) interlayer, which enabled covalent Michael-addition linking between MX surfaces and amine-MWCNTs [110]. This design produced a hierarchical, mechanically robust network with high surface area, excellent conductivity, and abundant exposed electroactive sites. The hybrid displayed outstanding electrocatalytic performance for acetaminophen detection, benefiting from the synergistic combination of MX's high electron mobility, the 1D conductive pathways of MWCNTs, and the strong interfacial adhesion provided by PDA. This materials strategy highlights three key principles: (i) construction of stable 2D/1D carbon-based hybrid networks, (ii) use of interfacial functional-linker chemistry to enhance mechanical and electrical integration, and (iii) maximization of accessible active sites for small-molecule sensing. Beyond PDA-modified MX structures, a hierarchical nanohybrid was further developed using molecularly imprinted polymer (MIP), Eu-MOF, PDA, Ti-MX, and Fe_3O_4 NPs for the ultrasensitive electrochemical detection of trimethylamine oxide, which is an important biomarker whose elevated levels are strongly linked to cardiovascular disease risk, gut microbiome dysregulation, and metabolic disorders [111]. The design began with PDA functionalization of Ti-MX, which prevented layer restacking and provided catechol and amine functional groups for strong interfacial coupling. A Eu-MOF was then hydrothermally grown on this 2D scaffold, forming columnar Eu-MOF structures intimately anchored to the PDA/MX matrix. The hybrid was subsequently integrated with Fe_3O_4 NPs, enabling uniform dispersion, facile magnetic-assisted electrode assembly, and improved mass transport. Finally, a MIP layer was electropolymerized onto the hybrid surface using catechol in the presence of trimethylamine oxide, generating highly specific recognition cavities. The resulting multifunctional nanohybrid delivered synergistic advantages: MX for high conductivity, PDA for structural stability, Eu-MOF for porosity and catalytic active sites, Fe_3O_4 for magnetic manipulation, and MIP for molecular specificity. This integrated architecture achieved exceptionally low femtomolar detection limits for trimethylamine oxide and demonstrated excellent accuracy in urine and plasma samples.

Building upon the use of single-metal MOFs, a bimetallic MOF was incorporated into MX to fabricate a dual-action MIP-based electrochemical sensor [112]. In this design, a hierarchical RGO/PDA/Ti-MX scaffold was integrated with a bimetallic FeCu-MOF to enable ultrasensitive detection of ribavirin, an antiviral drug whose excessive environmental or food-chain accumulation can contribute to antiviral resistance and pose hepatotoxic

and cardiotoxic risks. PDA-modified MX provided oxidation resistance, enhanced hydrophilicity, and prevented layer restacking, while RGO intercalation generated a stable 3D porous hetero-sheet that improved conductivity and electron transport. The FeCu-MOF contributed abundant catalytic sites, peroxidase-like activity, and a large electroactive surface area, enabling dual-signal readout through both $[Fe(CN)_6]^{3-/4-}$ redox cycling and H_2O_2 reduction. A computationally optimized o-phenylenediamine-based MIP was then electropolymerized to create high-affinity recognition cavities for ribavirin. The synergistic combination of MX stability, RGO conductivity, and MOF catalytic functionality resulted in exceptional sensitivity, selectivity, and strong performance in real sample analyses. In another study, an advanced sensing interface was developed using electrostatically assembled Ti-MX nanosheets incorporated with spherical $CuFe_2O_4$ magnetic nanospheres [113]. The magnetized hybrid was deposited onto a magnetic carbon paste electrode, improving dispersibility and interfacial conductivity. A MIP layer was then electropolymerized on top, specifically tailored for the flavonoid analyte quercetin, thereby generating high-affinity binding sites. Quercetin is an important bioflavonoid with antioxidant, anti-inflammatory, and anticancer properties, where its accurate detection in supplements and biological matrices is crucial for quality control and health evaluation. The hierarchical material design effectively leveraged MX's high conductivity and surface area, $CuFe_2O_4$'s magnetic responsiveness and catalytic potential, and the MIP's molecular specificity. The resulting sensor demonstrated excellent repeatability, selectivity, and stability in dietary supplement analysis. Similarly, a hybrid sensing interface was designed by anchoring Cu_xO nanostructures onto delaminated 2D Ti-MX sheets via in situ growth, forming a Cu_xO/MX composite with high conductivity and abundant catalytic sites [114]. Cu_xO provided redox-active centers for efficient melatonin oxidation, while the MX scaffold ensured rapid electron transfer, a large accessible surface area, and stable support for the recognition layer. In this regard, a MIP was electropolymerized using melatonin as the template, yielding highly selective binding cavities (Figure 6A). Melatonin is a key biomolecule regulating circadian rhythms and exhibiting antioxidant and anti-inflammatory functions; its precise quantification in biofluids is essential for diagnosing sleep disorders, monitoring neurodegenerative diseases, and supporting clinical evaluation. This hybrid architecture demonstrates the effectiveness of combining conductive 2D scaffolds, catalytic metal oxides, and imprinting polymers to achieve highly sensitive and selective analyte detection.

In another study, a hybrid electrode interface was constructed by in situ hydrothermal growth of nano-TiO_2 onto Ti-MX nanosheets to form a TiO_2/MX hybrid, which was subsequently functionalized with a MIP to create selective binding sites for levofloxacin [115]. Levofloxacin is a widely used fluoroquinolone antibiotic, and its excessive use contributes to environmental contamination and potential food-chain accumulation; therefore, ultrasensitive monitoring of its residues is essential for environmental and public health safety. The hybrid supported a robust platform for dense imprinting of polymeric recognition sites, demonstrating high binding affinity, good reproducibility, and long-term stability in real sample analyses. This material design highlights the synergistic contributions of 2D conductive MX, metal-oxide catalysis, and molecular imprinting in achieving selective and ultrasensitive detection of antibiotic residues.

Building on the benefits of metal-oxide integration, 2D Ti-MX nanosheets were further functionalized by covalently grafting first-generation PAMAM dendrimer to construct a PAMAM/MX hybrid architecture [116], as displayed in Figure 6B. The amine-rich branches of the PAMAM dendrimer offered abundant anchoring sites for self-assembled GNPs, yielding a 3D hierarchical GNPs/PAMAM/MX hybrid. This design retained the high conductivity and large surface area of MX while mitigating layer restacking and improving structural stability. The PAMAM dendrimer introduced plentiful functional groups for

biomolecule immobilization, whereas the GNPs enhanced electron transfer and facilitated efficient antibody loading. When implemented on a SPE, this hybrid enabled a label-free immunosensor for cardiac troponin T, a gold-standard biomarker for acute myocardial infarction, where rapid and sensitive detection is critical for timely diagnosis and clinical management of cardiovascular events.

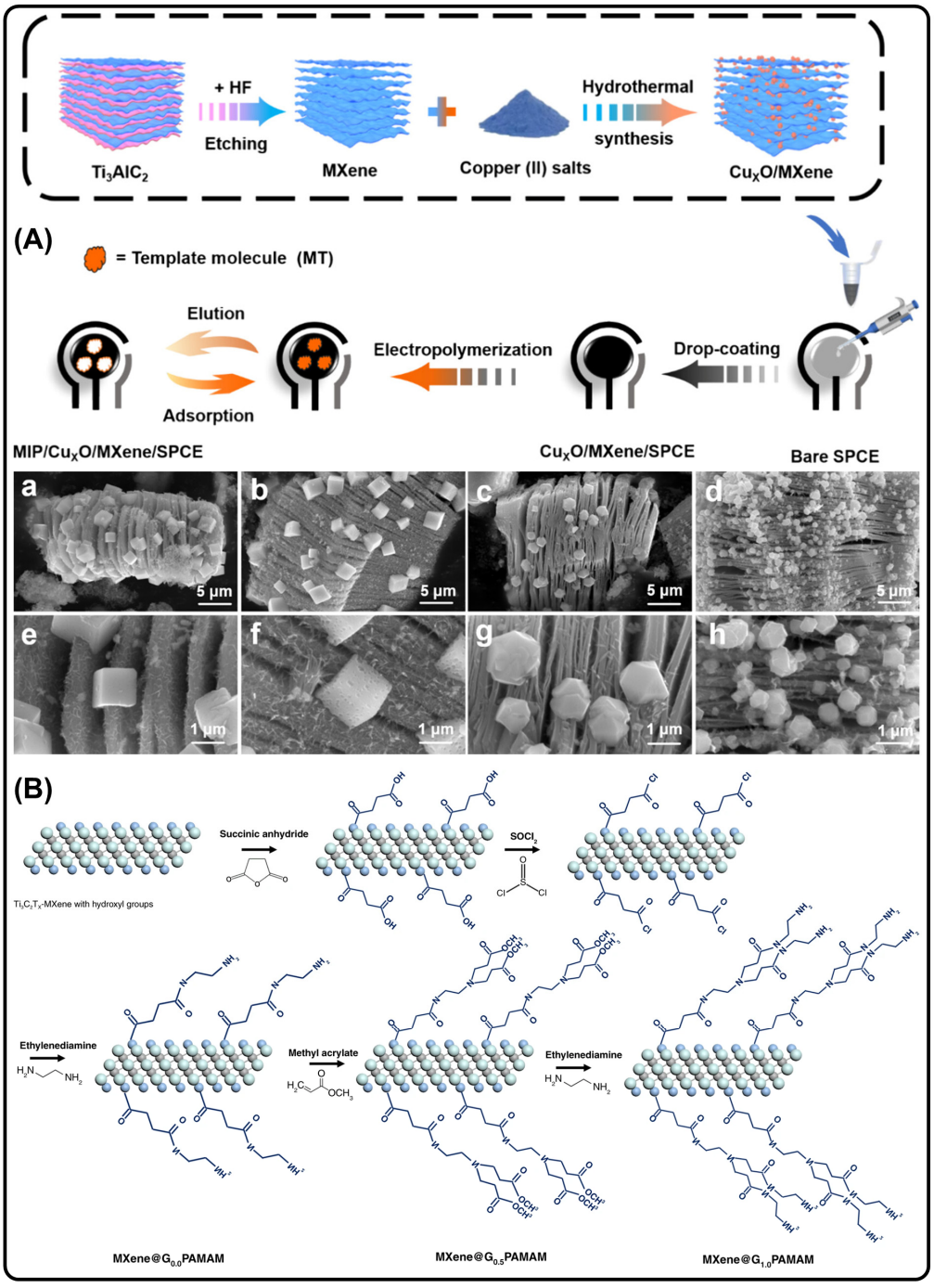

Figure 6. (**A**) Schematic illustration of the synthesis of Cu_XO/MX hybrid and the fabrication of MIP/Cu_XO/MX/SPE sensor. (**a**–**h**) SEM images of Cu_XO/MX prepared with different copper salts. Reproduced with permission from [114]. (**B**) Schematic representation of the stepwise synthesis of PAMAM dendrimer-decorated MX nanosheets. Reproduced with permission from [116].

To enhance the influence of the polymer component, a 2D Ti-MX was integrated with PEDOT, leveraging MX for its high conductivity and large surface area, and PEDOT

for improved stability and film-forming capability. In one study, a modifying ligand (4-sulfocalix[4]arene) and glucose oxidase enzyme were immobilized onto a PEDOT/MX film for the enzymatic detection of glucose [117]. In another, a plain PEDOT/MX film was employed for the nonenzymatic detection of thiocyanate [118]. The glucose sensor targeted a metabolite relevant to diabetes management and relies on enzyme specificity, whereas the thiocyanate sensor targeted an exposure-related biomarker ion and utilized the polymer-MX composite interface for amperometric sensing, demonstrating the versatility of the MX/PEDOT platform across both enzymatic and nonenzymatic modalities. From a materials perspective, the thiocyanate sensor represents a simplified design by eliminating enzyme immobilization and instead relying solely on the direct MX-polymer hybrid for analyte recognition, potentially offering greater robustness and operational simplicity.

Overall, MIP-based sensors exhibit high selectivity and stability for target analytes due to their tailor-made recognition sites, providing distinct advantages over conventional sensing approaches. The studies discussed above highlight diverse synthesis strategies, including electropolymerization and nanocomposite integration, which enhance surface area, electron-transfer kinetics, and binding affinity, ultimately enabling low detection limits and wide linear ranges. Table 5 compares the electrochemical performances of various MX-hybrid based MIP sensors. Compared with non-MIP or enzyme-free sensors previously described, MIP-based systems consistently demonstrate superior specificity and reusability, positioning them as promising candidates for practical implementation in biomedical, environmental, and food-monitoring applications.

Table 5. Electrochemical performance of different MX-hybrid MIP sensors.

Sensor	Analyte	Linear Range (μM)	LOD (μM)	Sensitivity	Real Sample	Ref.
NH_2-MWCNT/PDA/Ti-MX/GCE	Acetaminophen	10–60	0.01	-	Urine	[110]
Fe_3O_4/Eu-MOF/PDA@Ti-MX/GCE	Trimethylamine oxide	9×10^{-12}–9×10^{-9}	1.25×10^{-12}	63.73 μA M^{-1} cm^{-2}	Human plasma and urine	[111]
RPM/FeCu-MOF/GCE	Ribavirin	1×10^{-4}–5×10^{-4}	8.6×10^{-5}	-	River water, chicken, egg, milk	[112]
$CuFe_2O_4$/Ti-MX/MCPE	Quercetin	0.005–10	1.6×10^{-5}	-	Supplement capsule	[113]
Cu_xO/Ti-MX/SPCE	Melatonin	5–700	0.029	-	Human urine	[114]
TiO_2/Ti-MX/ITO	Levofloxacin	1×10^{-6}–1×10^{-1}	4.1×10^{-7}	5.804×10^{-5} μA μM^{-1} cm^{-2}	Human serum, urine, soil river water	[115]
PAMAM/Ti-MX/SPCE	Cardiac troponin T	* 0.1–1000	* 0.069	-	Human serum	[116]
GOx/PEDOT:SCX/Ti-MX/GCE	Glucose	5×10^2–8×10^3	22.5	-	Fruit juice	[117]
PEDOT/MX	Thiocyanate	0.1–1000	0.0325	0.0345 mA μM cm^{-2}	Sea and lake water, human saliva, artificial saliva	[118]

GOx—glucose oxidase; ITO—indium tin oxide; PAMAM—poly(amidoamine); PDA—polydopamine; PEDOT—poly(3,4-ethylenedioxythiophene); RPM—RGO/PDA@MX; SCX—4-sulfocalix[4]arene; *—ng mL^{-1}.

2.7. MXene Hybrids with Hydrogels

Hydrogels are three-dimensional polymeric networks formed through crosslinking, which provide them with unique properties such as high mechanical strength, high water content, excellent biocompatibility, and responsiveness to external stimuli, including pH, light, and temperature. Owing to these advantageous characteristics, hydrogels have found widespread applications across biomedical, agricultural, environmental, and food industries [119,120]. Incorporation of MX into hydrogels enhances their electrical conductivity and electrocatalytic activity, while the formation of MX-hydrogel hybrids improves the stability of MX, prevents interlayer restacking, increases biocompatibility, and enriches surface functionality. On the other hand, surface functionalization strategies may also reduce hydrophilicity, limit active surface terminations, and attenuate electrochemical activity arising from -OH and -O groups. Consequently, excessive or non-optimized functionalization can adversely affect analyte adsorption and interfacial charge transfer, underscoring the need for carefully balanced modification protocols.

A hydrogel composed of Ti-MX, TiO_2 NPs, GO and polyvinyl alcohol (PVA) was developed for the selective detection of urinary norepinephrine [121]. Norepinephrine is a key neurotransmitter involved in various physiological and pathological processes, including heart rate regulation, blood pressure control, stress response, and immune modulation; therefore, its selective detection is of significant clinical importance. In this study, Ti-MX was first synthesized and mixed with a TiO_2 sol, followed by incorporation into a preformed GO/PVA nanocomposite using a freeze–thaw method to obtain the final hydrogel. In the hybrid, TiO_2 improved the stability and reproducibility of MX, GO served as a nanofiller, and PVA contributed biocompatibility, low toxicity, and excellent water-absorption capability. The resulting sensor exhibited excellent performance in determining urinary norepinephrine, achieving good recovery values. Another neurotransmitter sensing platform was developed using a hydrogel composed of silane functionalized MX and poly(ethylene glycol)diacrylate (PEGDA) [122]. Initially, the MX nanosheets were silanized to enhance their stability and activity, after which they were mixed with PEGDA to form the hydrogel matrix (Figure 7A). This 3D nanostructure provided exceptional resistance to oxidation, improved mechanical robustness, and superior electrocatalytic activity compared to thin-film MX based sensors. The sensor successfully quantified dopamine, uric acid and serotonin with excellent sensitivity and selectivity.

A nonenzymatic glucose sensor was developed using a conductive hydrogel composed of Pt-decorated MX nanosheets [123]. PtNPs were synthesized in situ on the MX surface and subsequently mixed with PVA and sodium tetraborate to form the conductive hydrogel. The incorporation of PtNPs enhanced the stability of MX and significantly improved the electrocatalytic performance of the resulting glucose sensor. The hydrogel platform successfully quantified sweat glucose, as shown in Figure 7B. Another glucose sensing platform was fabricated using a hydrogel containing glucose oxidase encapsulated within a PEDOT:PSS-MX matrix [124]. The introduction of PEDOT:PSS improved the MX stability and provided a biocompatible microenvironment conducive to stable enzyme immobilization. Ethylene glycol was also incorporated during hydrogel formation to enhance electrical conductivity, porosity, and polymer expansion. The sensor's analytical performance closely matched that of a standard glucose meter. In parallel, a POC sensing system for continuous glucose monitoring was developed using a hydrogel containing PDA@MX nanosheets [125]. In this design, microneedles were coated with a hydrogel composed of PDA@MX and BSA crosslinked with glutaraldehyde to create an antibiofouling protective layer. This coating improved sensor stability and electrocatalytic activity during in vivo studies, and the obtained glucose measurements were comparable to those from handheld glucose meters.

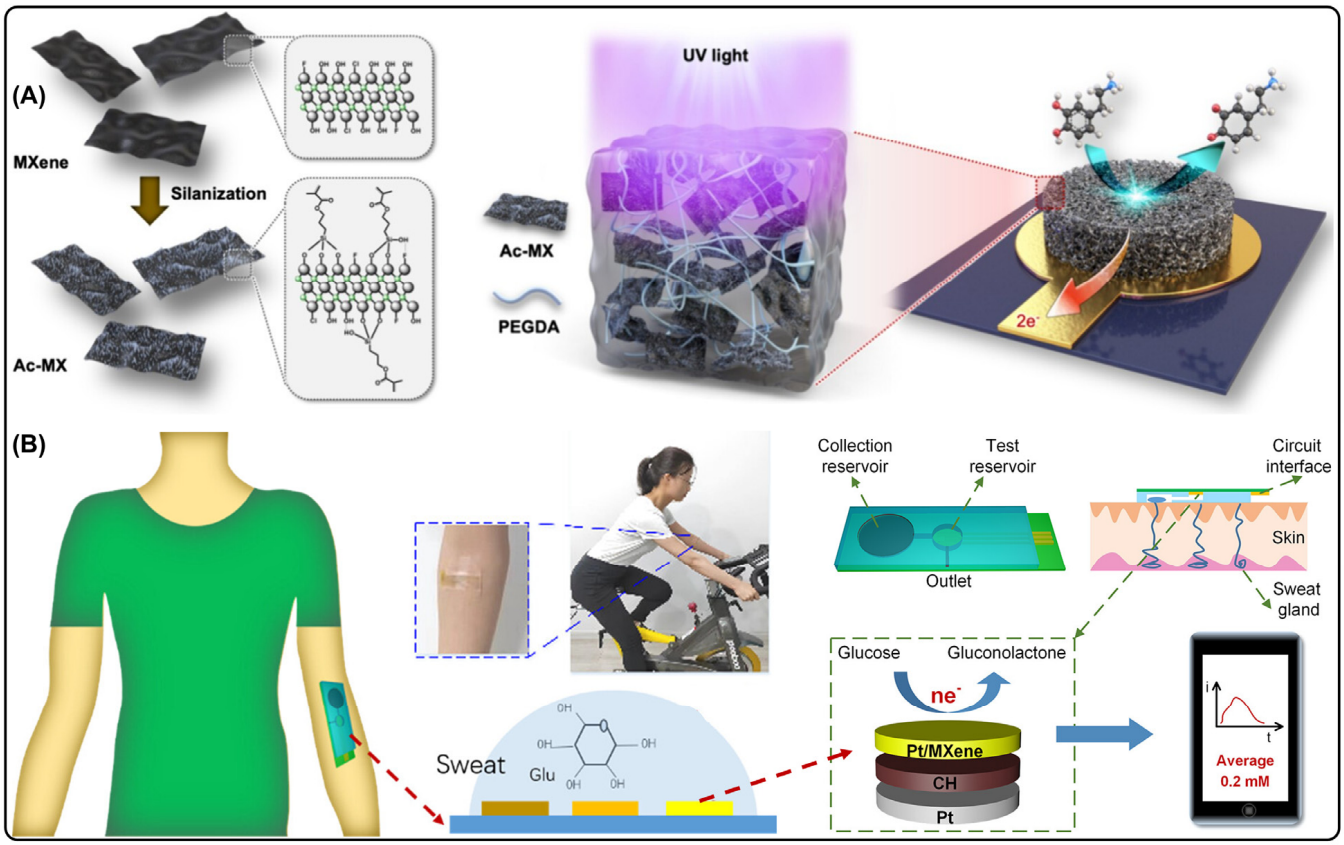

Figure 7. (**A**) Graphical representation of the synthesis of silane-functionalized MX-incorporated hydrogel and its electrocatalytic activity toward dopamine. Reproduced with permission from [122]. (**B**) Graphical illustration of the Pt-MX based hydrogel and its application in sweat-based glucose sensing. Reproduced with permission from [123].

A noninvasive, self-powered lactate sensor was developed using a hydrogel composed of MX nanosheets, enzymes, and polymer-modified carbon cloth [126]. Freshly prepared Ti-MX nanosheets were incorporated into a polypyrrole/polyurethane hydrogel matrix to improve their stability and electrical conductivity. In parallel, RGO decorated activated carbon cloth was functionalized with lactate oxidase and bilirubin oxidase and subsequently integrated with the Ti-MX/poly hydrogel. This hybrid configuration enabled lactate quantification without an external power source and exhibited a 15-fold enhancement in current response due to improved ionic and electronic conductivity. Another MX-incorporated polymer-based hydrogel with antifouling characteristics was developed for the sensitive detection of the tumor biomarker, carcinoembryonic antigen (CEA) [127]. In this approach, Ti-MX sheets were initially functionalized with carboxylic acid groups and a Ru complex, followed by silanization with KH570 to enhance dispersion stability. The modified MX sheets were then coated with a combination of monomers and polymers to improve antifouling property, stability, biocompatibility and surface functionality, thereby facilitating the effective immobilization of CEA-specific aptamer. The resulting sensor demonstrated excellent sensitivity toward CEA along with strong antifouling properties.

A MOF-incorporated vanadium carbide MX (VC-MX) hydrogel was developed for the simultaneous detection of levothyroxine and carbamazepine [128]. In this design, Co-MOF nanostructures were grown in situ on VC-MX nanosheets via a hydrothermal process followed by freeze-drying, and the resulting hybrid was mixed with PVA and Nafion to form the proposed hydrogel. Its highly porous and hydrophilic architecture provided a large surface area, enhanced electronic conductivity, and strong selectivity against common

interfering species. In another study, a disposable test strip sensor was fabricated for miRNAs detection using a Ti-MX aerogel decorated with GNPs and DNA hairpins on a carbon fiber paper [129]. The Ti-MX aerogel was prepared by mixing Ti-MX with GO and ethylene diamine to form a hydrogel, which upon freeze-drying, yielded the proposed aerogel. The resulting sensor showed excellent sensitivity, achieving attomolar detection limits. Similarly, a bacterial sensor for *Porphyromonas gingivalis* (PG) was developed using a multifunctional hydrogel (MHG) composed of VC-MX, GNPs, chitosan, pyrrole and ferrocene carboxaldehyde [130]. The MHG was deposited onto a gold electrode and sequentially functionalized with BSA and PG-specific antibodies. The sensor demonstrated outstanding activity toward PG detection, with performance comparable to that of an ELISA kit. A hydrogel with antifouling and antimicrobial properties was also constructed using amyloid albumin composites incorporated with cerium oxide NPs and Ti-MX nanosheets for wearable sweat-based dopamine sensing [131]. The amyloid albumin component enhanced the hydration layer, thereby reducing biofouling, while CeO_2 NPs contributed antimicrobial functionality. In another work, an estradiol sensor was fabricated using a nanoengineered hydrogel comprising MX and GNPs crosslinked with carboxymethyl chitosan and sodium carboxymethyl cellulose [132]. Ti-MX nanosheets were first synthesized and incorporated into the hydrogel matrix, followed by GNPs deposition and aptamer immobilization. The resulting sensor exhibited high porosity, good electrical conductivity, strong antifouling properties, and reliable performance in complex clinical samples. Table 6 compares the obtained electroanalytical performances of various MX-hybrid hydrogel based sensors.

Table 6. Electrochemical performance comparison of various MX-hydrogel based hybrids.

Sensor	Analyte	Linear Range (μM)	LOD (μM)	Sensitivity	Real Sample	Ref.
Tio_2/MX-PVA/GO/SPE	Norepinephrine	0.001–60	0.06	-	Urine samples	[121]
Si-MX-PEGDA/SPE	Dopamine	2.5–200	2.55	-	Human serum	[122]
	Uric acid	10–100	25.11			
	Serotonin	1–100	0.83			
Pt-MX-PVA/SPE	Glucose	0–8000	29.15	3.43 μA mM^{-1} cm^{-2}	Human sweat	[123]
GOx-MX-PEDOT:PSS/SPCE	Glucose	50–1300	1.9	21.7 μA mM^{-1} cm^{-2}	Human sweat	[124]
PDA@MX/MNs	Glucose	0–18 × 10^3	-	1.42 μA mM^{-1} cm^{-2}	Rat model	[125]
MX/Poly/RGO/CC	Lactate	1–50 × 10^3	-	-	Human sweat	[126]
Apt/PEDOT:PSS/MX/GCE	CEA	* 1–1 × 10^6	* 0.41	-	Human serum	[127]
Co-MOF/VC-MX	Levothyroxine	0.01–100	0.056	-	Simulated blood serum	[128]
	Carbamazepine	0.01–500	0.067	-		
GNPs/MX/CFP	miRNAs	20 × 10^{-9}–0.4	1.3 × 10^{-10}	-	Clinical samples	[129]
Ab/GNPs/VC-MX	*Porphyromonas gingivalis*	# 10–1 × 10^7	# 6	-	Saliva samples	[130]
AAHG/CeO/MX	Dopamine	0.05–300	0.017	-	Human sweat	[131]
Apt/GNPs/Ti-MX	Estradiol	* 0.1–1000	* 0.127		Human serum	[132]

AAHG—amyloid albumin hydrogel; Ab—antibody; Apt—Aptamer; CC—carbon cloth; CEA—carcinoembryonic antigen; CFP—carbon fiber paper; GNPs—gold nanoparticles; GOx—glucose oxidase; MNs—microneedles; MOF—metal–organic framework; PDA—polydopamine; PEGDA—poly(ethylene glycol)diacrylate; Poly—polypyrrole/polyurethane; PVA—polyvinyl alcohol; RGO—reduced graphene oxide; *—pg mL^{-1}; #—CFU mL^{-1}.

3. Conclusions and Future Outlook

MX-hybrids have rapidly emerged as one of the most versatile material platforms for electrochemical healthcare monitoring, driven by the synergistic integration of MX's exceptional conductivity and rich surface chemistry with the structural stability and complementary functionalities of polymers, nanoparticles, metal oxides, carbon allotropes, and biomolecules. This hybridization strategy significantly enhances sensitivity, selectivity, and operational robustness, enabling reliable detection of biomarkers, metabolites, pathogens, and therapeutic agents across a wide range of clinical and biomedical applications. The ability to rationally engineer hierarchical architecture and finely tailored interfaces has further expanded the design space for high-performance biosensors suitable for continuous monitoring, wearable and implantable diagnostics, and decentralized POC platforms.

Despite these strengths, several practical limitations continue to hinder the translation of MX-hybrids beyond laboratory-scale demonstrations. Key challenges include limited long-term chemical stability, susceptibility to oxidation, interfacial incompatibility, and difficulties associated with scalable and reproducible synthesis. Importantly, the future development of MX-hybrid-based electrochemical sensors must extend beyond performance optimization and explicitly address the fundamental trade-off between structural stabilization and intrinsic electrochemical activity. Similar compromises arise between maximizing surface functionalization and preserving electrical conductivity, as excessive surface modification or terminal-group capping can reduce hydrophilicity, restrict ion transport, and passivate electrochemically active sites, as well as between achieving ultrahigh sensitivity and ensuring the mechanical durability required for wearable or implantable applications. Moreover, device architecture and operating environment, particularly the distinction between dry thin-film sensors and continuously wetted or hydrogel-based systems, should guide material selection, surface functionalization, and stabilization strategies, as fluid-exposed architectures are inherently more susceptible to oxidative degradation [133,134]. Although many MX systems exhibit promising biocompatibility, long-term biosafety remains insufficiently understood, since degradation pathways may yield transition-metal oxides with markedly different toxicity profiles. From a safety standpoint, Ti-based MXenes currently appear more suitable for biointerfacing than V-based counterparts, given the higher toxicity associated with V_2O_5 formation upon degradation [135]. In addition, batch-to-batch variability in MX quality compromises reproducibility and poses challenges for regulatory approval and clinical standardization, while reliance on hazardous chemicals and harsh etchants during synthesis raises concerns regarding safety and environmental sustainability.

Future progress will depend on the development of robust stabilization strategies, scalable and environmentally benign synthesis routes, and hybrid architectures that balance sensing performance with manufacturability. Surface functionalization and hybridization approaches should therefore be critically assessed not only for their ability to suppress oxidation, but also for their influence on charge-transfer kinetics, accessible surface terminations, and long-term sensor reliability under realistic operating conditions. Looking ahead, the integration of MX-hybrid sensors with flexible electronics, machine-learning-assisted signal processing, and low-power edge computing offers a compelling pathway toward intelligent, real-time health-monitoring systems. Such convergence can transform raw electrochemical signals into clinically actionable information, enabling early disease detection, personalized therapy management, and improved patient outcomes [136,137]. Ultimately, bridging the gap between material innovation and real-world deployment will require coordinated efforts among materials scientists, engineers, clinicians, and data scientists, supported by rigorous long-term evaluations of stability, biocompatibility, and reliability. With these collective efforts, MX-hybrids are well-positioned to become founda-

tional components of next-generation healthcare technologies that are accurate, accessible, and equitable.

Author Contributions: Conceptualization, K.T. and Y.-J.K.; methodology, K.T. and Y.-J.K.; validation, K.T. and Y.-J.K.; formal analysis, K.T. and Y.-J.K.; resources, Y.-J.K.; data curation, K.T. and Y.-J.K.; writing—original draft preparation, K.T.; writing—review and editing, K.T. and Y.-J.K.; visualization, K.T.; supervision, Y.-J.K.; project administration, Y.-J.K.; funding acquisition, Y.-J.K. All authors have read and agreed to the published version of the manuscript.

Funding: This work was funded by the National Research Foundation of Korea (Grant numbers: RS-2025-24683075, RS-2024-00433166).

Institutional Review Board Statement: Not applicable.

Informed Consent Statement: Not applicable.

Data Availability Statement: No data were used for the research described in the article.

Acknowledgments: The icons used in the graphical abstract were adapted from flaticon.com and BioRender. Kim, Y. (2025) https://BioRender.com/kji08fy, accessed on 20 November 2025.

Conflicts of Interest: The authors declare no conflicts of interest.

Abbreviations

2D	Two-dimensional
3D	Three-dimensional
AAHG	Amyloid albumin hydrogel
Ab	Antibody
Apt	Aptamer
APTES	(3-Aminopropyl)triethoxysilane
AuE	Gold electrode
BC	Bacterial cellulose
BCD	Beta–Cyclodextrin
CB	Carbon black
CC	Carbon cloth
CEA	Carcinoembryonic antigen
CFP	Carbon fiber paper
CNs	Carbon nanostructures
CNT	Carbon nanotubes
COF	Covalent organic framework
CYFRA21–1	Cytokeratin fragment antigen 21–1
DAAQ	2,6-Diaminoanthraquinone
DNA	Deoxyribonucleic acid
ELISA	Enzyme linked immunosorbent assays
Glu	Glutamate
GNPs	Gold nanoparticles
GNU	Gold nanourchins
GO	Graphene oxide
GOx	Glucose oxidase
GR	Graphene
HCP	Hydrophobic carbon paper
h–MWCNT	Holey multiwalled carbon nanotubes
LIG	Laser induced graphene
LSG	Laser–scribed graphene
MHG	Multifunctional hydrogel
MIP	Molecular imprinted polymer

MNs	Microneedles
MOFs	Metal–organic frameworks
MX	MXenes
NPs	Nanoparticles
PAMAM	Polyamidoamine
PDA	Polydopamine
PEGDA	Poly(ethylene glycol) diacrylate
PEI	Polyethyleneimine
PG	*Porphyromonas gingivalis*
POC	Point-of-care
Poly	Polypyrrole/polyurethane
PtNPs	Platinum nanoparticles
PVA	Polyvinyl alcohol
RGO	Reduced graphene oxide
SeNPs	Selenium nanoparticles
SPCE	Screen printed carbon electrode
SWCNT	Single walled carbon nanotubes
TB	Toluidine blue
xGnP	Exfoliated graphite nanoplates
ZIF	Zeolitic imidazolate framework

References

1. Mirlou, F.; Beker, L. Wearable Electrochemical Sensors for Healthcare Monitoring: A Review of Current Developments and Future Prospects. *IEEE Trans. Mol. Biol. Multi-Scale Commun.* **2023**, *9*, 364–373. [CrossRef]
2. Vo, D.-K.; Trinh, K.T.L. Advances in Wearable Biosensors for Healthcare: Current Trends, Applications, and Future Perspectives. *Biosensors* **2024**, *14*, 560. [CrossRef]
3. Ameen, S.S.M.; Omer, K.M.; Mansour, F.R.; Bedair, A.; Hamed, M. Non-Invasive Wearable Electrochemical Sensors for Continuous Glucose Monitoring. *Electrochem. Commun.* **2025**, *173*, 107894. [CrossRef]
4. Sanko, V.; Tekin, H.C. Electrochemical Sensors for Rapid Cardiovascular Disease Diagnostics. *ACS Sens.* **2025**, *10*, 6316–6346. [CrossRef]
5. Singh, S.; Glovi, A.; Miglione, A.; Cimmino, W.; Iula, G.; Antonelli, L.; De Cesaris, M.G.; Felli, N.; Martinelli, C.; De Laurentiis, M.; et al. Electrochemical (Bio)Sensors for Cancer Therapy Monitoring. *Electrochim. Acta* **2025**, *537*, 146929. [CrossRef]
6. Bae, M.; Kim, N.; Cho, E.; Lee, T.; Lee, J.-H. Recent Advances in Electrochemical Biosensors for Neurodegenerative Disease Biomarkers. *Biosensors* **2025**, *15*, 151. [CrossRef]
7. Sinha, R. The Role and Impact of New Technologies on Healthcare Systems. *Discov. Health Syst.* **2024**, *3*, 96. [CrossRef]
8. Yu, Y.; Jain, B.; Anand, G.; Heidarian, M.; Lowe, A.; Kalra, A. Technologies for Non-Invasive Physiological Sensing: Status, Challenges, and Future Horizons. *Biosens. Bioelectron. X* **2024**, *16*, 100420. [CrossRef]
9. Theyagarajan, K.; Zahra, L.; Kim, Y.-J. Advances in the Design and Fabrication of Flexible, Wearable, and Implantable Electrochemical Neurotransmitter Sensors. *Coord. Chem. Rev.* **2026**, *549*, 217287. [CrossRef]
10. Thanjavur, N.; Bugude, L.; Kim, Y.-J. Integration of Functional Materials in Photonic and Optoelectronic Technologies for Advanced Medical Diagnostics. *Biosensors* **2025**, *15*, 38. [CrossRef] [PubMed]
11. Srinivas, S.; Sekar, M.; Thirumurugan, K.; Senthil Kumar, A. Hemozoin Anchored MWCNTs for Mediated Reduction of Hydrogen Peroxide and Real-Time Intracellular Oxidative Stress Monitoring in Colon Cancer Cells. *J. Mater. Chem. B* **2025**, *13*, 985–996. [CrossRef]
12. Saikrithika, S.; Kim, Y.-J. Biochar-Derived Electrochemical Sensors: A Green Route for Trace Heavy Metal Detection. *Chemosensors* **2025**, *13*, 278. [CrossRef]
13. Theyagarajan, K.; Kim, Y.-J. Metal Organic Frameworks Based Wearable and Point-of-Care Electrochemical Sensors for Healthcare Monitoring. *Biosensors* **2024**, *14*, 492. [CrossRef]
14. Wilkirson, E.C.; Singampalli, K.L.; Li, J.; Dixit, D.D.; Jiang, X.; Gonzalez, D.H.; Lillehoj, P.B. Affinity-Based Electrochemical Sensors for Biomolecular Detection in Whole Blood. *Anal. Bioanal. Chem.* **2023**, *415*, 3983–4002. [CrossRef]
15. Theyagarajan, K.; Lakshmi, B.A.; Kim, Y.-J. Enzymeless Detection and Real-Time Analysis of Intracellular Hydrogen Peroxide Released from Cancer Cells Using Gold Nanoparticles Embedded Bimetallic Metal Organic Framework. *Colloids Surf. B Biointerfaces* **2025**, *245*, 114209. [CrossRef]

16. Lin, J.; Chen, Y.; Liu, X.; Jiang, H.; Wang, X. Engineered Intelligent Electrochemical Biosensors for Portable Point-of-Care Diagnostics. *Chemosensors* **2025**, *13*, 146. [CrossRef]
17. Gao, F.; Liu, C.; Zhang, L.; Liu, T.; Wang, Z.; Song, Z.; Cai, H.; Fang, Z.; Chen, J.; Wang, J.; et al. Wearable and Flexible Electrochemical Sensors for Sweat Analysis: A Review. *Microsyst. Nanoeng.* **2023**, *9*, 1. [CrossRef]
18. Sanli, S. Single-Drop Electrochemical Immunosensor with 3D-Printed Magnetic Attachment for Onsite Smartphone Detection of Amoxicillin in Raw Milk. *Food Chem.* **2024**, *437*, 137823. [CrossRef]
19. Theyagarajan, K.; Kim, Y.-J. Recent Developments in the Design and Fabrication of Electrochemical Biosensors Using Functional Materials and Molecules. *Biosensors* **2023**, *13*, 424. [CrossRef]
20. Pradhan, S.; Albin, S.; Heise, R.L.; Yadavalli, V.K. Portable, Disposable, Biomimetic Electrochemical Sensors for Analyte Detection in a Single Drop of Whole Blood. *Chemosensors* **2022**, *10*, 263. [CrossRef]
21. Baranwal, J.; Barse, B.; Gatto, G.; Broncova, G.; Kumar, A. Electrochemical Sensors and Their Applications: A Review. *Chemosensors* **2022**, *10*, 363. [CrossRef]
22. Munteanu, I.G.; Apetrei, C. A Review on Electrochemical Sensors and Biosensors Used in Assessing Antioxidant Activity. *Antioxidants* **2022**, *11*, 584. [CrossRef]
23. Thanjavur, N.; Kim, Y.-J. Illuminating Pollutants: The Role of Carbon Dots in Environmental Sensing. *Chemosensors* **2025**, *13*, 241. [CrossRef]
24. Srinivas, S.; Sivakumar, N.; Sekar, M.; Thirumurugan, K.; Senthil Kumar, A. Benzene Layer-Aligned Electrochemical Transformation of SWCNTs to Redox-Active Macro-Walled CNTs: Enabling Oxygen Interference-Free Monitoring of ROS Release from HeLa Cancer Cells. *J. Mater. Chem. C* **2024**, *12*, 11885–11897. [CrossRef]
25. Irfan Azizan, M.A.; Taufik, S.; Norizan, M.N.; Abdul Rashid, J.I. A Review on Surface Modification in the Development of Electrochemical Biosensor for Malathion. *Biosens. Bioelectron. X* **2023**, *13*, 100291. [CrossRef]
26. Pimpilova, M. A Brief Review on Methods and Materials for Electrode Modification: Electroanalytical Applications towards Biologically Relevant Compounds. *Discov. Electrochem.* **2024**, *1*, 12. [CrossRef]
27. Lutomia, D.; Poria, R.; Kala, D.; Garg, P.; Nagraik, R.; Kaushal, A.; Gupta, S.; Kumar, D. 2D Nanomaterials in Biosensing: Synthesis, Characterization, Integration in Biosensors and Their Applications. *Biosens. Bioelectron. X* **2025**, *24*, 100615. [CrossRef]
28. Masud; Song, J.; Ahmed, F.; Kim, J. 2D Materials: From Design and Synthesis to Applications in Electrical and Electrochemical Biosensors. *Small* **2025**, *21*, e04955. [CrossRef]
29. Yang, M.; Fu, D.; Gao, C.; Liu, Y. 2D Material-Based Electrochemical Sensors for Early Diabetes Detection: A Review of Progress and Prospects. *Int. J. Electrochem. Sci.* **2025**, *20*, 101123. [CrossRef]
30. Ullah, S.; Nazir, M.A.; Saeed, M.A.; Ullah, S.; Hossain, I.; Assiri, M.A.; Tamang, T.L.; Janušas, G. Next Generation MXene Based Materials for Electrochemical Sensor: A Critical Review. *J. Mol. Struct.* **2025**, *1321*, 139830. [CrossRef]
31. Yang, M.; Xie, C.; Lu, H. Advances in MXene-Based Electrochemical Sensors for Multiplexed Detection in Biofluids. *Int. J. Mol. Sci.* **2025**, *26*, 5368. [CrossRef]
32. Gogotsi, Y.; Anasori, B. The Rise of MXenes. *ACS Nano* **2019**, *13*, 8491–8494. [CrossRef]
33. Mohanapriya, D.; Satija, J.; Senthilkumar, S.; Kumar Ponnusamy, V.; Thenmozhi, K. Design and Engineering of 2D MXenes for Point-of-Care Electrochemical Detection of Bioactive Analytes and Environmental Pollutants. *Coord. Chem. Rev.* **2024**, *507*, 215746. [CrossRef]
34. Sun, M.; Ye, W.; Zhang, J.; Zheng, K. Structure, Properties, and Preparation of MXene and the Application of Its Composites in Supercapacitors. *Inorganics* **2024**, *12*, 112. [CrossRef]
35. Loganathan, H.; Dhinasekaran, D.; Rajendran, A.R. Recent Advances in MXene-Based Electrochemical Sensors for Healthcare Applications. *TrAC Trends Anal. Chem.* **2025**, *189*, 118276. [CrossRef]
36. Cao, W.; Nie, J.; Cao, Y.; Gao, C.; Wang, M.; Wang, W.; Lu, X.; Ma, X.; Zhong, P. A Review of How to Improve $Ti_3C_2T_x$ MXene Stability. *Chem. Eng. J.* **2024**, *496*, 154097. [CrossRef]
37. Jangra, S.; Kumar, B.; Sharma, J.; Sengupta, S.; Das, S.; Brajpuriya, R.K.; Ohlan, A.; Mishra, Y.K.; Goyat, M.S. A Review on Overcoming Challenges and Pioneering Advances: MXene-Based Materials for Energy Storage Applications. *J. Energy Storage* **2024**, *101*, 113810. [CrossRef]
38. Bi, W.; Gao, G.; Li, C.; Wu, G.; Cao, G. Synthesis, Properties, and Applications of MXenes and Their Composites for Electrical Energy Storage. *Prog. Mater. Sci.* **2024**, *142*, 101227. [CrossRef]
39. Aravind, A.M.; Tomy, M.; Kuttapan, A.; Kakkassery Aippunny, A.M.; Suryabai, X.T. Progress of 2D MXene as an Electrode Architecture for Advanced Supercapacitors: A Comprehensive Review. *ACS Omega* **2023**, *8*, 44375–44394. [CrossRef]
40. Alagarsamy, K.N.; Saleth, L.R.; Diedkova, K.; Zahorodna, V.; Gogotsi, O.; Pogorielov, M.; Dhingra, S. MXenes in Healthcare: Transformative Applications and Challenges in Medical Diagnostics and Therapeutics. *Nanoscale* **2025**, *17*, 11785–11811. [CrossRef]
41. Sundaram, A.; Ponraj, J.S.; Wang, C.; Peng, W.K.; Manavalan, R.K.; Dhanabalan, S.C.; Zhang, H.; Gaspar, J. Engineering of 2D Transition Metal Carbides and Nitrides MXenes for Cancer Therapeutics and Diagnostics. *J. Mater. Chem. B* **2020**, *8*, 4990–5013. [CrossRef]

42. Iravani, S.; Varma, R.S. MXenes for Cancer Therapy and Diagnosis: Recent Advances and Current Challenges. *ACS Biomater. Sci. Eng.* **2021**, *7*, 1900–1913. [CrossRef]
43. Maduraiveeran, G.; Jin, W. Carbon Nanomaterials: Synthesis, Properties and Applications in Electrochemical Sensors and Energy Conversion Systems. *Mater. Sci. Eng. B* **2021**, *272*, 115341. [CrossRef]
44. Ahmad, H.; Khan, R.A.; Koo, B.H.; Alsalme, A. Systematic Study of Physicochemical and Electrochemical Properties of Carbon Nanomaterials. *RSC Adv.* **2022**, *12*, 15593–15600. [CrossRef]
45. Solangi, N.H.; Karri, R.R.; Mubarak, N.M.; Mazari, S.A.; Sharma, B.P. Holistic Insights into Carbon Nanotubes and MXenes as a Promising Route to Bio-Sensing Applications. *Nanoscale* **2024**, *16*, 21216–21263. [CrossRef]
46. Shi, S.; Zhong, R.; Li, L.; Wan, C.; Wu, C. Ultrasound-Assisted Synthesis of graphene@MXene Hybrid: A Novel and Promising Material for Electrochemical Sensing. *Ultrason. Sonochem.* **2022**, *90*, 106208. [CrossRef]
47. Gu, H.; Xing, Y.; Xiong, P.; Tang, H.; Li, C.; Chen, S.; Zeng, R.; Han, K.; Shi, G. Three-Dimensional Porous $Ti_3C_2T_x$ MXene–Graphene Hybrid Films for Glucose Biosensing. *ACS Appl. Nano Mater.* **2019**, *2*, 6537–6545. [CrossRef]
48. Rajendran, J.; Sundramoorthy, A.K.; Ganapathy, D.; Atchudan, R.; Habila, M.A.; Nallaswamy, D. 2D MXene/Graphene Nanocomposite Preparation and Its Electrochemical Performance towards the Identification of Nicotine Level in Human Saliva. *J. Hazard. Mater.* **2022**, *440*, 129705. [CrossRef]
49. Rajendran, J.; Kannan, T.S.; Dhanasekaran, L.S.; Murugan, P.; Atchudan, R.; ALOthman, Z.A.; Ouladsmane, M.; Sundramoorthy, A.K. Preparation of 2D Graphene/MXene Nanocomposite for the Electrochemical Determination of Hazardous Bisphenol A in Plastic Products. *Chemosphere* **2022**, *287*, 132106. [CrossRef]
50. Baumgarten, L.G.; Dreyer, J.P.; De Campos, C.E.M.; Germano, A.T.; Vitali, L.; Spinelli, A.; Santana, E.R.; Winiarski, J.P.; Vieira, I.C. Two-Dimensional Titanium Carbide MXene Embedded in Exfoliated Graphite Nanoplatelets for Voltammetric Sensing of Thiamethoxam in Beekeeping Products. *Electrochim. Acta* **2024**, *494*, 144423. [CrossRef]
51. Wei, K.; Pan, K.; Qu, G.; Qin, J.; Lv, J.; Liang, Y. Self-Assembly of GO-MXene Hybrid Composites by Polyelectrolyte: As an Efficient Electrocatalyst for Selective Electrochemical Detection of the Antibiotic Furazolidone. *J. Environ. Chem. Eng.* **2024**, *12*, 112319. [CrossRef]
52. Jiang, M.; Tian, L.; Su, M.; Cao, X.; Jiang, Q.; Huo, X.; Yu, C. Real-Time Monitoring of 5-HT Release from Cells Based on MXene Hybrid Single-Walled Carbon Nanotubes Modified Electrode. *Anal. Bioanal. Chem.* **2022**, *414*, 7967–7976. [CrossRef]
53. Gurbuz, H.N.; Tok, K.C.; Gumustas, M.; Cagil, E.M.; Ipekci, H.H.; Uzunoglu, A. Development of Flexible Nicotine Sensors by Inkjet Printing of Heteroatom-Doped 3D V2C MXene Nanoflower/Holey Carbon Nanotube-Based Inks. *FlatChem* **2025**, *49*, 100811. [CrossRef]
54. Zhang, S.; Zahed, M.A.; Sharifuzzaman, M.; Yoon, S.; Hui, X.; Chandra Barman, S.; Sharma, S.; Yoon, H.S.; Park, C.; Park, J.Y. A Wearable Battery-Free Wireless and Skin-Interfaced Microfluidics Integrated Electrochemical Sensing Patch for on-Site Biomarkers Monitoring in Human Perspiration. *Biosens. Bioelectron.* **2021**, *175*, 112844. [CrossRef]
55. Ranjith, K.S.; Mohammadi, A.; Ezhil Vilian, A.T.; Han, S.; Huh, Y.S.; Han, Y.-K. Synergistic Effects of CNT-Bridged Dual-Phase MoS_2 on MXene as a Ternary Hybrid Electrode for Rapid Sensing of Chloramphenicol in Aqueous Media. *Chem. Eng. J.* **2024**, *500*, 157487. [CrossRef]
56. Chavan, S.G.; Rathod, P.R.; Koyappayil, A.; Karuppaiah, G.; Go, A.; Jin, E.; Park, J.; Lee, M.-H. Self-Assembled AuNPs on Niobium Carbide (Nb_2C) MXene-Based Apta-Sensor for Progesterone Recognition in Female Sweat and Serum Sample. *Sens. Actuators B Chem.* **2025**, *437*, 137722. [CrossRef]
57. Li, Q.; Ren, J.; Feng, K.; Gong, J.; Li, Z.; Liu, X.; Zhang, J. An Electrochemical Sensor Based on MXene-Au Nanocomposites/Janus Fiber Membrane for Sweat Glucose Detection via Rapid Unidirectional Moisture Transport Collection. *Talanta* **2026**, *298*, 128819. [CrossRef]
58. Nandi, I.; Kumari, R.; Kachhawaha, K.; Singh, S.K.; Chandra, P. Electrochemical Sensor Based on a MXene Nanosheet–Gold Nanourchin Hybrid as a Superoxide Dismutase Mimic for Real-Time Detection of Superoxide Anions Released from Living Cells. *ACS Appl. Nano Mater.* **2024**, *7*, 12171–12183. [CrossRef]
59. Tu, W.; Sun, M.; Lu, T.; Chen, Y.; Zhou, Y.; Zhang, C.; Ni, Z.; Li, X.; Hu, T. Wearable Electrochemical Aptasensor Based on MXene@gold Nanoparticles for Non-Invasive Sweat Cortisol Detection. *Biosens. Bioelectron.* **2025**, *287*, 117736. [CrossRef]
60. Cheng, J.; Hu, K.; Liu, Q.; Liu, Y.; Yang, H.; Kong, J. Electrochemical Ultrasensitive Detection of CYFRA21-1 Using $Ti_3C_2T_x$-MXene as Enhancer and Covalent Organic Frameworks as Labels. *Anal. Bioanal. Chem.* **2021**, *413*, 2543–2551. [CrossRef]
61. Lv, Y.; Zhou, Y.; Dong, H.; Xu, M.; Zhang, J.; Yan, M. Ultrasensitive Electrochemical Detection of Amyloid-Beta Oligomers Using Double Amplification Strategy by MXene Substrate and Covalent Organic Framework-Based Probe. *Talanta* **2024**, *266*, 125134. [CrossRef]
62. Mi, X.; Li, H.; Tan, R.; Feng, B.; Tu, Y. The TDs/Aptamer cTnI Biosensors Based on HCR and Au/Ti_3C_2-MXene Amplification for Screening Serious Patient in COVID-19 Pandemic. *Biosens. Bioelectron.* **2021**, *192*, 113482. [CrossRef]
63. Wang, W.; Yin, Y.; Gunasekaran, S. Gold Nanoparticles-Doped MXene Heterostructure for Ultrasensitive Electrochemical Detection of Fumonisin B1 and Ampicillin. *Microchim. Acta* **2024**, *191*, 294. [CrossRef]

64. Chen, Y.; Zhang, X.; Liu, Y.; Liu, Z.; Li, Z.; Li, Z.; Chen, X.; Liu, J.; Chen, Z.; Mo, G.; et al. A Gold Nanoparticles and MXene Nanocomposite Based Electrochemical Sensor for Point-of-Care Monitoring of Serum Biomarkers. *ACS Nano* **2025**, *19*, 16980–16994. [CrossRef]
65. Wang, Y.; Zhao, P.; Gao, B.; Yuan, M.; Yu, J.; Wang, Z.; Chen, X. Self-Reduction of Bimetallic Nanoparticles on Flexible MXene-Graphene Electrodes for Simultaneous Detection of Ascorbic Acid, Dopamine, and Uric Acid. *Microchem. J.* **2023**, *185*, 108177. [CrossRef]
66. Lorencova, L.; Bertok, T.; Filip, J.; Jerigova, M.; Velic, D.; Kasak, P.; Mahmoud, K.A.; Tkac, J. Highly Stable $Ti_3C_2T_x$ (MXene)/Pt Nanoparticles-Modified Glassy Carbon Electrode for H_2O_2 and Small Molecules Sensing Applications. *Sens. Actuators B Chem.* **2018**, *263*, 360–368. [CrossRef]
67. Kumar, A.S.; Saikrithika, S.; Yesudas, Y.K. In Situ Prussian Blue-Electrocatalyst Formation on Intrinsic Iron-Containing Pristine-MWCNT as a Template and Its EQCM and SECM Interrogations and Batch Injection Analysis of Hydrogen Peroxide. *J. Electrochem. Soc.* **2023**, *170*, 056507. [CrossRef]
68. De Lima, L.F.; Ferreira, A.L.; Dos Santos, L.E.; Coelho, K.L.P.; Santos, K.T.; Schmidt, A.; De Jesus, M.B.; Paixão, T.R.L.C.; De Araujo, W.R. Bacterial Cellulose-Based Laser-Scribed Graphene Electrode for Hydrogen Peroxide Detection in Cancer Cells. *ACS Appl. Bio Mater.* **2025**, *8*, 6339–6349. [CrossRef]
69. Liu, X.; Chen, L.; Yang, Y.; Xu, L.; Sun, J.; Gan, T. MXene−reinforced Octahedral PtCu Nanocages with Boosted Electrocatalytic Performance towards Endocrine Disrupting Pollutants Sensing. *J. Hazard. Mater.* **2023**, *442*, 130000. [CrossRef]
70. Zhang, W.; Wang, Y.; Hu, Z. Electrochemically Assembled MXene/Ni Hybrid Interfaces for Non-Enzymatic Glucose Sensing: Toward Smart Salivary Diagnostics. *Mater. Sci. Eng. B* **2025**, *321*, 118515. [CrossRef]
71. Prabisha, K.E.; Neena, P.K.; Ankitha, M.; Rasheed, P.A.; Suneesh, P.V.; Satheesh Babu, T.G. Selenium Nanoparticles Modified Niobium MXene for Non-Enzymatic Detection of Glucose. *Sci. Rep.* **2025**, *15*, 1749. [CrossRef]
72. Asaduzzaman, M.; Lee, Y.Y.; Samad, A.A.; Reza, M.S.; Kim, D.Y.; Islam, Z.; Park, J.Y. MXene@Pt Nanocomposite and Nanoporous Carbon Reinforced 3D Graphene-Based Electrochemical Multi-Sensing Patch for Wearable Sweat Analysis. *Chem. Eng. J.* **2025**, *514*, 163292. [CrossRef]
73. Qu, G.; Zhang, Y.; Zhou, J.; Tang, H.; Ji, W.; Yan, Z.; Pan, K.; Ning, P. Simultaneous Electrochemical Detection of Dimethyl Bisphenol A and Bisphenol A Using a Novel Pt@SWCNTs-MXene-rGO Modified Screen-Printed Sensor. *Chemosphere* **2023**, *337*, 139315. [CrossRef]
74. Tawalbeh, M.; Khan, H.A.; Al-Othman, A. Insights on the Applications of Metal Oxide Nanosheets in Energy Storage Systems. *J. Energy Storage* **2023**, *60*, 106656. [CrossRef]
75. Raj, M.K.A.; Rathanasamy, R.; Kumar, P.M.; M, D.; Kaliyannan, G.V.; Alam, M.M.; Keçebaş, A. Synergistic Integration of Transition Metal Oxides and Conducting Polymers for High-Performance Supercapacitors: Advances, Challenges, and Future Prospects. *Surf. Interfaces* **2025**, *78*, 108117. [CrossRef]
76. Mathew, S.; Sunajadevi, K.R.P.; Pinheiro, D. Transition Metal Oxide/Chalcogenide-Integrated MXene Heterostructures: Emerging Materials for Supercapacitors and Water Splitting. *Mater. Adv.* **2025**, *6*, 7207–7230. [CrossRef]
77. Zermane, M.; Teniou, A.; Berkani, M.; Sobti, N.; Catanante, G.; Gnanasekaran, L.; Vasseghian, Y.; Rhouati, A. MXene ($Ti_3C_2T_x$)-Fe_2O_3 Hybrid Nanomaterials for Electrochemical Ultra-Sensitive Testosterone Detection. *ACS Appl. Nano Mater.* **2025**, *8*, 5611–5622. [CrossRef]
78. Yazdanian, M.; Sabeti, B.; Chekin, F. Magnetite MXene-Based Hybrid Platforms for Electrochemical Sensing of Anticancer Drug Idarubicin. *J. Electron. Mater.* **2025**, *54*, 1645–1652. [CrossRef]
79. Ilanchezhiyan, P.; Manikandan, R.; Sekar, S.; Jin Lee, D.; Chang Jeon, H.; Lee, S.; Chang, S.-C.; Young Kim, D. Two Dimensional $FeVO_4$ Nanoflakes Decorated on Ti_3C_2 MXene Hybrid Nanocomposites as a Novel Effective Electrochemical Biosensor for Ultrasensitive and Selective Detection of Serotonin (5-HT). *Appl. Surf. Sci.* **2025**, *680*, 161411. [CrossRef]
80. Ranjith, K.S.; Vilian, A.T.E.; Ghoreishian, S.M.; Umapathi, R.; Huh, Y.S.; Han, Y.-K. An Ultrasensitive Electrochemical Sensing Platform for Rapid Detection of Rutin with a Hybridized 2D-1D MXene-$FeWO_4$ Nanocomposite. *Sens. Actuators B Chem.* **2021**, *344*, 130202. [CrossRef]
81. Wang, Y.; Fu, K.; Zhang, Y. A Flexible Carbonized Rice-Paper-Based Electrode by Layer-by-Layer Assembly of Few-Layer $Ti_3C_2T_x$ and ZIF-67 Microcubes for Wearable Electrochemical Sweat Lactate Sensing. *Sens. Actuators B Chem.* **2025**, *444*, 138455. [CrossRef]
82. Varatharajan, P.; Rajaji, U.; Vasimalai, N.; Chung, R.-J.; Liu, T.-Y. A Wide Linear Range and Highly Sensitive Electrochemical Reduction of Environmental Hazard (p-Nitrotoluene) Using Carbon-Based Hybrid Composite ($Ti_3C_2T_X$@$MnCo_2O_4$). *J. Environ. Chem. Eng.* **2024**, *12*, 114301. [CrossRef]
83. Subramania, A.K.; Sugumaran, S.; Sethuramalingam, P.; Ramesh, R.; Dhandapani, P.; Angaiah, S. $NiCo_2O_4$/Ti_2NbC_2 (Double MXene) Nanohybrid-Based Non-Enzymatic Electrochemical Biosensor for the Detection of Glucose in Sweat. *Bioprocess Biosyst. Eng.* **2023**, *46*, 1755–1763. [CrossRef] [PubMed]

84. Waris, M.H.; Muzaffar, N.; Mumtaz, M.A.; Afzal, A.M.; Iqbal, M.W.; Mumtaz, S.; Ali, M.; Alaraidh, I.A.; Okla, M.K.; Munnaf, S.A. High Performance Lanthanum-Doped Nickel Cobalt Ferrites on Titanium Carbide MXene Electrode Material for Superior Hybrid Device and Precision Creatinine Sensing. *Appl. Phys. A* **2025**, *131*, 220. [CrossRef]
85. Ranjith, K.S.; Ezhil Vilian, A.T.; Ghoreishian, S.M.; Umapathi, R.; Hwang, S.-K.; Oh, C.W.; Huh, Y.S.; Han, Y.-K. Hybridized 1D–2D $MnMoO_4$–MXene Nanocomposites as High-Performing Electrochemical Sensing Platform for the Sensitive Detection of Dihydroxybenzene Isomers in Wastewater Samples. *J. Hazard. Mater.* **2022**, *421*, 126775. [CrossRef] [PubMed]
86. Baskaran, N.; Prasanna, S.B.; Jeyaram, K.; Lin, Y.-C.; Govindasamy, M.; Wei, Y.; Chung, R.-J. 2D Sheet Structure of Zinc Molybdate Decorated on MXene for Highly Selective and Sensitive Electrochemical Detection of the Arsenic Drug Roxarsone in Water Samples. *Chemosphere* **2024**, *364*, 143188. [CrossRef]
87. Anupriya, J.; Senthilkumar, T.; Chen, S.M. A Precise Electrochemical Sensor Based on Sm_2O_3/2D TiC Hybrid for Highly Sensitive and Selective Detection of Antihypertensive Drug Nimodipine. *Colloids Surf. A Physicochem. Eng. Asp.* **2022**, *641*, 128531. [CrossRef]
88. Liu, G.; Xia, T.; Liang, X.; Hou, S.; Hou, S. Enzymatic Electrochemical Biosensor from Eu-Doped SnO_2 Embedded in MXene for High Performance Sensing Lactate. *ChemElectroChem* **2022**, *9*, e202200848. [CrossRef]
89. Cheng, H.; Zhang, L.; Feng, J.; Tang, T.; Qin, D. A Novel Sensor Based on Ti_3C_2 MXene/Co_3O_4/Carbon Nanofibers Composite for the Sensitive Detection of 4-Aminophenol. *Chemosphere* **2023**, *341*, 139981. [CrossRef]
90. An, J.; Luo, M.; Li, M.; Cui, H.; Liu, Y. Development of an Advanced Electrochemical Biosensor for Choline Detection Using MXene, MWCNT-AuNPs, and Fe_3O_4NPs. *Microchem. J.* **2025**, *214*, 114034. [CrossRef]
91. Sahadevan, K.; Vinoba, M.; Revathi, S.; Jeong, S.K.; Bhagiyalakshmi, M. Facile Design of NiO-rGO/$Mo_2Ti_2C_3$ Ternary Composites for Electrochemical Detection of Dopamine. *Synth. Met.* **2025**, *312*, 117876. [CrossRef]
92. Mohan, B.; Dhiman, D.; Virender; Mehak; Priyanka; Sun, Q.; Jan, M.; Singh, G.; Raghav, N. Metal-Organic Frameworks (MOFs) Structural Properties and Electrochemical Detection Capability for Cancer Biomarkers. *Microchem. J.* **2023**, *193*, 108956. [CrossRef]
93. Rodrigues, P.; Bangali, H.; Saleh, E.A.M.; Hamza, S.R.; Mirzaev, B.S.; Ghali, F.; Hussien, B.M.; Hussein, S.B.; Habash, R.T.; Mustafa, Y.F. Metal-Organic Framework/MXene Nanohybrid Composites as an Emerging Electrochemical Sensing Platform for Food Safety and Biomedical Monitoring: From Synthesis to Application. *Electrochim. Acta* **2024**, *494*, 144424. [CrossRef]
94. Roy, D.; Singh, R.; Mandal, S.; Chanda, N. An MXene-Supported Cobalt-MOF Nanocomposite-Printed Electrochemical Sensor with High Sensitivity for Blood Creatinine Detection in Point-of-Care Settings. *Anal. Methods* **2024**, *16*, 6183–6192. [CrossRef] [PubMed]
95. Zhang, N.; Bao, R.; Jia, H.; Zhang, E.; Zheng, S.; Tang, J.; Wang, X.; Wang, W.; Guo, J. 3D ZIF-67 Dodecahedral Embedded in 2D MXene Nanosheets for Electrochemical Determination of Dopamine. *Microchem. J.* **2025**, *216*, 114661. [CrossRef]
96. Shen, B.; Hong, B.; Guo, X.; Hu, R.; Wang, L.; Jiang, Y.; Li, W.; Liu, W.; Wu, Z.; Yang, P. Facile Fabrication of Sensing Electrode Based on CoFe-MOFs/MXene for Ultrasensitive Detection of Picomolar Chloramphenicol. *Talanta* **2025**, *286*, 127552. [CrossRef]
97. Richard, B.; Niyas, K.; Ankitha, M.; Rasheed, P.A. Biological Metal–Organic Framework-Embedded MXene Nanocomposite as a Wearable Transducer Patch for Real-Time Monitoring of the Sleep Hormone. *ACS Appl. Nano Mater.* **2024**, *7*, 9585–9597. [CrossRef]
98. Daniel, M.; Rafi, J.; Reza, S.; Thapa, R.; Mathur, S.; Neppolian, B. Enhancing Host-Guest Interactions through Interfacial Modulation of IRMOF-MXene Hybrids: A Detailed Study on the Significance of Accessible Functional Groups in Electrochemical Detection. *Mater. Res. Bull.* **2025**, *192*, 113611. [CrossRef]
99. Zhao, K.; Zhang, B.; Cui, X.; Chao, X.; Song, F.; Chen, H.; He, B. An Electrochemical Aptamer-Sensing Strategy Based on a $Ti_3C_2T_x$ MXene Synergistic Ti-MOF Amplification Signal for Highly Sensitive Detection of Zearalenone. *Food Chem.* **2024**, *461*, 140828. [CrossRef]
100. Kaur, G.; Sharma, S.; Bhardwaj, N.; Nayak, M.K.; Deep, A. Highly Sensitive and Selective Electrochemical Detection of Aflatoxin B1 in Water and Pistachio Samples with MOF/MXene Composite Based Sensor. *Food Control* **2024**, *165*, 110694. [CrossRef]
101. Afzal, M.H.; Pervaiz, W.; Huang, Z.; Wang, Z.; Li, G.; Liu, H. In Situ Synthesis of a UIO-66-NH_2 @Ti_3C_2Composite for Advanced Electrochemical Detection of Acetaminophen. *Nanoscale* **2025**, *17*, 4444–4454. [CrossRef]
102. Saikrithika, S.; Senthil Kumar, A. In Situ Electrochemical Trapping and Unraveling the Mechanism of the Toxic Intermediate Metabolite *N*-Acetyl-*p*-Benzoquinone Imine of the Acetaminophen Drug and Its Biomimetic Mediated NADH Oxidation Reaction. *J. Phys. Chem. C* **2023**, *127*, 8016–8029. [CrossRef]
103. Zhang, Y.; Cao, T.; Bai, B.; Jing, X.; Yu, L.; Zhang, J.; Bo, T.; Liu, H.; Gu, Y.; Yang, Y. Ultra-Sensitive and Rapid Detection of Diethylstilbestrol by Constructing Molecularly Imprinted Electrochemical Sensor via Hetero-Interface Engineering of Pt Nanoparticles-Decorated MXene/NH_2-UiO-66. *Food Chem.* **2025**, *493*, 146061. [CrossRef] [PubMed]
104. Yusran, Y.; Miao, B.; Qiu, S.; Fang, Q. Functional Covalent Organic Frameworks: Design Principles to Potential Applications. *Acc. Mater. Res.* **2024**, *5*, 1263–1278. [CrossRef]
105. Valentini, C.; Montes-García, V.; Pakulski, D.; Samorì, P.; Ciesielski, A. Covalent Organic Frameworks and 2D Materials Hybrids: Synthesis Strategies, Properties Enhancements, and Future Directions. *Small* **2025**, *21*, 2410544. [CrossRef]

106. Punniyamoorthy, M.; Soosaimanickam, C.; Kathiresan, M.; Alwarappan, S. 2D Nb_2C MXene/COF Composite as Electrochemical Platform for the Stress Marker Epinephrine Detection. *ACS Appl. Nano Mater.* **2025**, *8*, 19771–19778. [CrossRef]
107. Yang, Z.; Guo, H.; Sun, L.; Yu, Z.; Yang, W. Self-Referenced Ratiometric Electrochemical Biosensor Based on Covalent Organic Framework Assembled MXene for Stain-Resistance and Sensitive Sensing of Dopamine. *Talanta* **2026**, *297*, 128614. [CrossRef]
108. Fei, Q.; Huang, Q.; Nie, D.; Fan, K.; Wang, X.; Bian, M.; Zhao, Z.; Han, Z. A Host–Guest Recognition Electrochemical Sensor Based on MXene/COF Heterocomposite Bound to β-Cyclodextrin for the Direct Detection of Zearalenone in Cereals. *Microchem. J.* **2025**, *213*, 113887. [CrossRef]
109. Yan, R.; Guo, H.; Yang, Z.; Niu, W.; Ma, J.; Peng, L.; Wang, M.; Yang, W. Construction of a Purine Base Electrochemical Sensing Platform Based on NH_2-MXene@COFTA-DH/GCE for Simultaneous Detection of Guanine and Adenine. *Colloids Surf. A Physicochem. Eng. Asp.* **2025**, *714*, 136572. [CrossRef]
110. Chen, S.; Xu, J.; Shi, M.; Yu, Y.; Xu, Q.; Duan, X.; Gao, Y.; Lu, L. Polydopamine Bridged MXene and NH_2-MWCNTs Nanohybrid for High-Performance Electrochemical Sensing of Acetaminophen. *Appl. Surf. Sci.* **2021**, *570*, 151149. [CrossRef]
111. Liang, X.; Yan, Y.; Liu, G.; Hou, S.; Hou, S. Constructing Magnetically Functionalized Sandwich-like Eu-MOF/PDA@MXene Hybrids for Extremely Sensitive Molecular Imprinted Sensor toward Trace Detecting Trimethylamine Oxide. *Chem. Eng. J.* **2024**, *483*, 149301. [CrossRef]
112. Gao, H.; You, J.; Wu, H.; Tian, M. A Dual Action Electrochemical Molecular Imprinting Sensor Based on FeCu-MOF and RGO/PDA@MXene Hybrid Synergies for Trace Detection of Ribavirin. *Food Chem.* **2025**, *473*, 143092. [CrossRef]
113. Ganjeh, A.A.; Arvand, M.; Habibi, M.F. Electrostatically Self-Assembled Magnetized MXene/Copper Ferrite Nanospheres Hybrids: Evaluation of Molecularly Imprinted Electrochemical Sensor for the Quercetin Antioxidant Supplement. *Microchem. J.* **2024**, *207*, 112026. [CrossRef]
114. Wang, X.; Wang, W.; Gao, M.; Yu, H.; Fu, M.; Chen, W. Molecularly Imprinted Electrochemical Sensor Based on Cu_xO/MXene Nanocomposite for Sensing of Melatonin. *ACS Appl. Nano Mater.* **2024**, *7*, 22832–22842. [CrossRef]
115. Hudda, D.; Kumar, D. Titanium Dioxide Grafted MXene-Based Molecularly Imprinted Electrochemical Sensor for the Ultrasensitive Determination of Levofloxacin. *J. Solid State Electrochem.* **2025**, *29*, 5283–5295. [CrossRef]
116. Liu, X.; Qiu, Y.; Jiang, D.; Li, F.; Gan, Y.; Zhu, Y.; Pan, Y.; Wan, H.; Wang, P. Covalently Grafting First-Generation PAMAM Dendrimers onto MXenes with Self-Adsorbed AuNPs for Use as a Functional Nanoplatform for Highly Sensitive Electrochemical Biosensing of cTnT. *Microsyst. Nanoeng.* **2022**, *8*, 35. [CrossRef]
117. Murugan, P.; Annamalai, J.; Atchudan, R.; Govindasamy, M.; Nallaswamy, D.; Ganapathy, D.; Reshetilov, A.; Sundramoorthy, A.K. Electrochemical Sensing of Glucose Using Glucose Oxidase/PEDOT:4-Sulfocalix [4]Arene/MXene Composite Modified Electrode. *Micromachines* **2022**, *13*, 304. [CrossRef]
118. Rajendran, J. Amperometric Determination of Salivary Thiocyanate Using Electrochemically Fabricated Poly (3,4-Ethylenedioxythiophene)/MXene Hybrid Film. *J. Hazard. Mater.* **2023**, *449*, 130979. [CrossRef]
119. Mahinroosta, M.; Jomeh Farsangi, Z.; Allahverdi, A.; Shakoori, Z. Hydrogels as Intelligent Materials: A Brief Review of Synthesis, Properties and Applications. *Mater. Today Chem.* **2018**, *8*, 42–55. [CrossRef]
120. Li, N.; He, J. Hydrogel-Based Therapeutic Strategies for Spinal Cord Injury Repair: Recent Advances and Future Prospects. *Int. J. Biol. Macromol.* **2024**, *277*, 134591. [CrossRef]
121. Boobphahom, S.; Siripongpreda, T.; Zhang, D.; Qin, J.; Rattanawaleedirojn, P.; Rodthongkum, N. TiO_2/MXene-PVA/GO Hydrogel-Based Electrochemical Sensor for Neurological Disorder Screening via Urinary Norepinephrine Detection. *Microchim. Acta* **2021**, *188*, 387. [CrossRef]
122. Mun, T.J.; Yang, E.; Moon, J.; Kim, S.; Park, S.G.; Kim, M.; Choi, N.; Lee, Y.; Kim, S.J.; Seong, H. Silane-Functionalized MXene-PEGDA Hydrogel for Enhanced Electrochemical Sensing of Neurotransmitters and Antioxidants. *ACS Appl. Polym. Mater.* **2024**, *6*, 9533–9544. [CrossRef]
123. Li, Q.-F.; Chen, X.; Wang, H.; Liu, M.; Peng, H.-L. Pt/MXene-Based Flexible Wearable Non-Enzymatic Electrochemical Sensor for Continuous Glucose Detection in Sweat. *ACS Appl. Mater. Interfaces* **2023**, *15*, 13290–13298. [CrossRef]
124. Pan, Y.; He, M.; Wu, J.; Qi, H.; Cheng, Y. One-Step Synthesis of MXene-Functionalized PEDOT:PSS Conductive Polymer Hydrogels for Wearable and Noninvasive Monitoring of Sweat Glucose. *Sens. Actuators B Chem.* **2024**, *401*, 135055. [CrossRef]
125. Tong, X.; Jiang, T.; Yang, J.; Song, Y.; Ao, Q.; Tang, J.; Zhang, L. Continuous Glucose Monitoring (CGM) System Based on Protein Hydrogel Anti-Biofouling Coating for Long-Term Accurate and Point-of-Care Glucose Monitoring. *Biosens. Bioelectron.* **2025**, *277*, 117307. [CrossRef]
126. Xiao, D.; Zou, M.; Huang, M. Wearable Self-Powered Electrochemical Sensor with MXene/PU Composite and Advanced Electrodes for Non-Invasive Lactate Detection during Physical Activity. *Mater. Sci. Eng. B* **2025**, *322*, 118647. [CrossRef]
127. Geng, F.; Li, Y.; Wu, Q.; Ding, C. An Efficient Electrochemical Biosensor Based on Double-Conductive Hydrogel as Antifouling Interface for Ultrasensitive Analysis of Biomarkers in Complex Serum Medium. *Sens. Actuators B Chem.* **2025**, *422*, 136625. [CrossRef]

128. Ravipati, M.; Ramasamy, D.; Badhulika, S. Highly Selective Cobalt-MOF/Vanadium Carbide MXene Hydrogel for Simultaneous Electrochemical Determination of Levothyroxine and Carbamazepine in Simulated Blood Serum. *Electrochim. Acta* **2025**, *525*, 146154. [CrossRef]
129. Yang, H.; Wen, L.; Wang, X.; Zhao, J.; Dong, J.; Yin, X.; Xu, F.; Yang, M.; Huo, D.; Hou, C. A Test Strip Electrochemical Disposable by 3D MXA/AuNPs DNA-Circuit for the Detection of miRNAs. *Microchim. Acta* **2022**, *189*, 50. [CrossRef]
130. Shen, H.; Fu, Y.; Liu, Z.; Pan, S.; Zhou, F.; Peng, Y.; Yang, X.; Zhang, X.; Song, J. A Handheld Electrochemical Bacterial Sensor Based on Multifunctional Composite Hydrogels and DNA Biomimetic Nanowalls for Accurate Detection of *Porphyromonas gingivalis*. *Chem. Eng. J.* **2024**, *498*, 155344. [CrossRef]
131. Song, Z.; Li, R.; Li, Z.; Luo, X. Antifouling and Antimicrobial Wearable Electrochemical Sweat Sensors for Accurate Dopamine Monitoring Based on Amyloid Albumin Composite Hydrogels. *Biosens. Bioelectron.* **2024**, *264*, 116640. [CrossRef]
132. Karuppaiah, G.; Koyappayil, A.; Chavan, S.G.; Go, A.; Seowoo, H.; Rathod, P.R.; Lee, S.; Lee, M.-H. Nanoengineered Hybrid Hydrogel-Based 3D Nanocomposite as an Antifouling Coating Interface for Enhanced Electrochemical Aptasensing of Estradiol. *Talanta* **2025**, *293*, 128105. [CrossRef]
133. Ramezani Farani, M.; Mirzaee, D.; Hatami, A.; Kumar, K.; Ghoreishian, S.M.; Huh, Y.S. Biocompatibility and Immunomodulation of MXenes for Targeted Delivery of Bioactive Agents and Drugs. *Bioact. Mater.* **2026**, *55*, 546–567. [CrossRef] [PubMed]
134. Sankar, S.N.; Araujo, G.; Fernandes, J.; Cerqueira, F.; Alpuim, P.; Ribeiro, A.R.; Lebre, F.; Alfaro-Moreno, E.; Placidi, E.; Marras, S.; et al. Eco-Friendly Production of 2D $Ti_3C_2T_x$ MXene and Cytotoxicity Mitigation Toward Biomedical Applications. *Adv. Mater. Inter.* **2024**, *11*, 2400203. [CrossRef]
135. Jastrzębska, A.M.; Scheibe, B.; Szuplewska, A.; Rozmysłowska-Wojciechowska, A.; Chudy, M.; Aparicio, C.; Scheibe, M.; Janica, I.; Ciesielski, A.; Otyepka, M.; et al. On the Rapid in Situ Oxidation of Two-Dimensional V_2CTz MXene in Culture Cell Media and Their Cytotoxicity. *Mat. Sci. Eng. C* **2021**, *119*, 111431. [CrossRef]
136. Kim, Y.-J.; Kwon, Y.; Yoo, Y.; Theyagarajan, K.; Saikrithika, S.; Lee, A.; Bae, N.H.; Lee, W.-C.; Sim, G.; Lee, Y.; et al. Demonstration of CMOS-Compatible Memristor-Based Electrochemical Biosensor Transducer with Threshold-Sensing Functionality. *Nat. Commun.* **2025**, *16*, 10851. [CrossRef] [PubMed]
137. Li, Y.; Liu, D.; Meng, S.; Chen, T.; Liu, C.; You, T. Dual-Ratiometric Electrochemical Aptasensor Enabled by Programmable Dynamic Range: Application for Threshold-Based Detection of Aflatoxin B1. *Biosens. Bioelectron.* **2022**, *195*, 113634. [CrossRef] [PubMed]